ACS APPLIED MATERIALS & INTERFACES

Review

www.acsami.org

Graphitic Carbon Nitride: Synthesis, Properties, and Applications in Catalysis

Junjiang Zhu,*[,†] Ping Xiao,[†] Hailong Li,[†] and Sónia A. C. Carabineiro[‡]

[†]Key Laboratory of Catalysis and Materials Science of the State Ethnic Affairs & Commission Ministry of Education, South-Central University for Nationalities, Wuhan 430074, China

[‡]Laboratory of Catalysis and Materials (LCM), Associate Laboratory (LSRE/LCM), Department of Chemical Engineering, Faculty of Engineering, University of Porto, Rua Dr. Roberto Frias, 4200-465 Porto, Portugal

ABSTRACT: Graphitic carbon nitride, g-C_3N_4, is a polymeric material consisting of C, N, and some impurity H, connected via tris-triazine-based patterns. Compared with the majority of carbon materials, it has electron-rich properties, basic surface functionalities and H-bonding motifs due to the presence of N and H atoms. It is thus regarded as a potential candidate to complement carbon in material applications. In this review, a brief introduction to g-C_3N_4 is given, the methods used for synthesizing this material with different textural structures and surface morphologies are described, and its physicochemical properties are referred. In addition, four aspects of the applications of g-C_3N_4 in catalysis are discussed: (1) as a base metal-free catalyst for NO decomposition, (2) as a reference material in differentiating oxygen activation sites for oxidation reactions over supported catalysts, (3) as a functional material to synthesize nanosized metal particles, and (4) as a metal-free catalyst for photocatalysis. The reasons for the use of g-C_3N_4 for such applications are also given, and we expect that this paper will inspire readers to search for further new applications for this material in catalysis and in other fields.

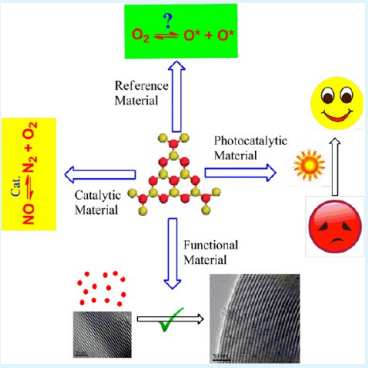

KEYWORDS: *graphitic carbon nitride, synthesis, physicochemical properties, applications, metal-free catalyst, reference material, functional material*

1. INTRODUCTION

Carbon nitrides are a class of polymeric materials consisting mainly of carbon and nitrogen.[1,2] They can be obtained from carbon materials, through substitution of the carbon atoms by nitrogen, and become appealing candidates for a variety of applications. Like most carbon materials, carbon nitrides also have a long history, which can be traced back to 1834, when a material prepared by Berzelius was named "melon" (linear polymers of connected tri-s-triazines via secondary nitrogen), and reported by Liebig.[3] However, the potential value of this material was not fully recognized until recent decades, most likely because of its chemical inertness, insolubility in acidic, neutral or basic solvents, and its unrevealed structure.[4]

Graphitic carbon nitride (g-C_3N_4) is not only the most stable allotrope of carbon nitrides at ambient atmosphere, but it also has rich surface properties that are attractive for many applications, including catalysis, due to the presence of basic surface sites. The ideal g-C_3N_4 consists solely of an assembly of C−N bonds without electron localization in the π state (this material is a π-conjugated polymer).[6] Real materials, like those prepared by polycondensation of cyanamide, contain a small amount of hydrogen, present as primary and/or secondary amine groups on the terminating edges, as seen in Figure 1.[3] The existence of hydrogen indicates that the real g-C_3N_4 is incompletely condensed and that a number of surface defects exist, which can be useful in catalysis, for example, and are believed to promote electron relocalization on the surface,

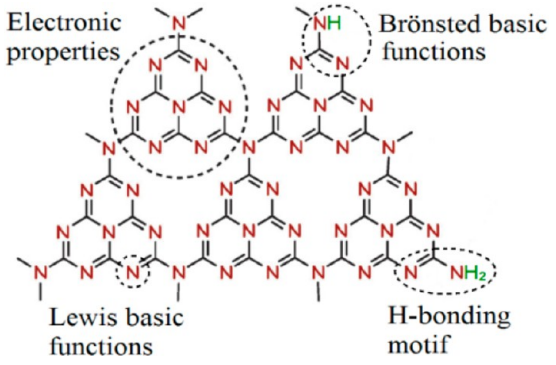

Figure 1. Multiple surface functionalities found on g-C_3N_4. Reprinted with permission from ref 5. Copyright 2008 Royal Society of Chemistry.

inducing Lewis-base character toward metal-free coordination chemistry and catalysis.

Because of the presence of hydrogen and tothe fact that nitrogen has one more electron than carbon, g-C_3N_4 has rich surface properties that are important to catalysis, such as basic surface functionalities, electron-rich properties, H-bonding

Received: May 13, 2014
Accepted: September 12, 2014
Published: September 12, 2014

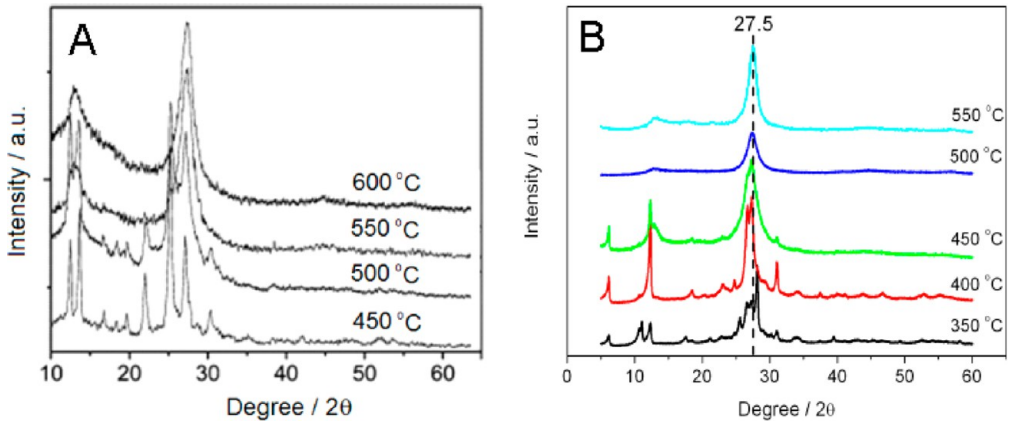

Figure 2. XRD patterns of g-C_3N_4 synthesized from cyanamide at different temperatures. (A) Cyanamide was used as received. Reprinted with permission from ref 5. Copyright 2008 Royal Society of Chemistry. (B) Cyanamide was pretreated with a NaOH solution.

motifs, etc., as shown in Figure 1. Moreover, its high thermal stability (it is stable up to 600 °C in air)[7] and hydrothermal stability (it is insoluble either in acidic, neutral or basic solvents)[8] enables the material to function either in liquid or gaseous environments, and at elevated temperatures, potentiating its wide applications in heterogeneous catalysis. Indeed, it has been reported that g-C_3N_4 is a promising catalyst for various reactions, including CO_2 activation,[9,10] transesterification,[11] oxygen reduction,[12,13] hydrogen production,[8,14−16] photodegradation of dyes,[17] etc. Several reviews reporting the catalytic performances of g-C_3N_4 in a variety of reactions can be found elsewhere.[4,18−21]

This work overviews the recent advances of g-C_3N_4 in three aspects, based on the results obtained by the authors, as well as those from literature: (1) comparison of the reported preparation methods by a condensation route; (2) discussion of the thermal behavior and surface basicity of materials prepared using different conditions; (3) description of several interesting uses of g-C_3N_4 in catalysis, already reported by the authors and in the literature, and the reasons why g-C_3N_4 has been used for such applications. This review also aims to provide basic knowledge in the synthesis of g-C_3N_4 samples with different properties and inspire the readers to seek new applications of these materials in catalysis or material sciences.

2. SYNTHESIS

The most common precursors used for chemical synthesis of g-C_3N_4 are reactive nitrogen-rich and oxygen-free compounds containing prebonded C−N core structures, such as triazine and heptazine derivatives, most of them being unstable, difficult to obtain and/or highly explosive. The synthesis of single-phase sp^3-hybridized carbon nitrides is a challenging task due to their low thermodynamic stability.[22,23] Not surprisingly, it seems that the defect materials are much more valuable than the ideal one, in particular for catalysis, which requires surface defects. Thus, the synthesis of g-C_3N_4 with defects is an interesting topic, when the material is going to be used in catalysis.

The condensation pathways from cyanamide to Dicyandiamide, and to melamine and all other C/N materials are simple and good synthetic routes to generate slightly defected polymeric species.[5] The cyanamide precursor is finally transformed to g-C_3N_4 at ca. 550 °C, as confirmed by XRD (Figure 2A), with consequent formation of NH_3. The synthesis can be conducted either in inert (e.g., N_2, Ar) or in air atmosphere, with no significant changes in the bulk structure; but may lead to differences in the product yield, degree of condensation and, especially, surface properties, which will be described in detail in the following section.

In order to promote the condensation process and lower the condensation temperature, the synthesis should be conducted in a basic environment. Pure g-C_3N_4 is obtained at ca. 500 °C when the precursor cyanamide is pretreated with a basic solution (like aqueous NaOH), as confirmed by XRD (Figure 2B). This indicates that the presence of hydroxyl ions facilitates the transformation of cyanamide to g-C_3N_4, probably due to the hydroxyl ions that promote the condensation process, by reacting with the hydrogen atoms on the edges of the intermediate. The reduction of the condensation temperature promotes some properties, like the surface area of the material, because of less aggregation.

However, cyanamide is expensive and explosive,[24,25] and the solubility of its derivates (dicyanamide or melamine) is low, therefore the synthesis of g-C_3N_4 with the desired (e.g., porous) structures, using these precursors, is either expensive or hard to operate. To overcome this limitation, Xu et al. reported the use of guanidine hydrochloride (GndCl), which is a water-soluble, environmentally friendly, and cheap material, as a precursor, to synthesize g-C_3N_4.[25] They found that the material can be produced by direct condensation of the GndCl in Ar atmosphere at 550 °C for 3 h, which is similar to the procedure operated using cyanamide as precursor. Similar to that reported for cyanamide, the condensation of GndCl occurs by the transformation of melamine to melem, polymeric melem, and finally to g-C_3N_4, with subsequent release of NH_3.

The surface area of g-C_3N_4 prepared by direct polycondensation of C-, N-, and H-containing precursors is normally low (ca. 10 m^2/g),[8] because of the graphitic layered structure. This limits the performances of g-C_3N_4 in heterogeneous catalysis, since surface reactions require the catalyst to exhibit a certain surface area, to adsorb and activate the substrate. In order to overcome this limitation, g-C_3N_4 can be deposited on a high surface area material, like SBA-15.[27] As g-C_3N_4 is a polymeric material, it can coat or spread on the support surface forming a film layer with increased surface area. Wang et al. reported that Fe incorporated g-C_3N_4 (Fe-*g*-C_3N_4) can be homogeneously coated on SBA-15 (Figure 3) by an impregnation method, with a surface area increase from 8 to 506 m^2/g.[26] The activity raised from 0 (for Fe-*g*-C_3N_4) to 15 h^{-1} (for Fe-*g*-C_3N_4/SBA-15), in terms of TOF, for the photocatalytic oxidation of benzene to

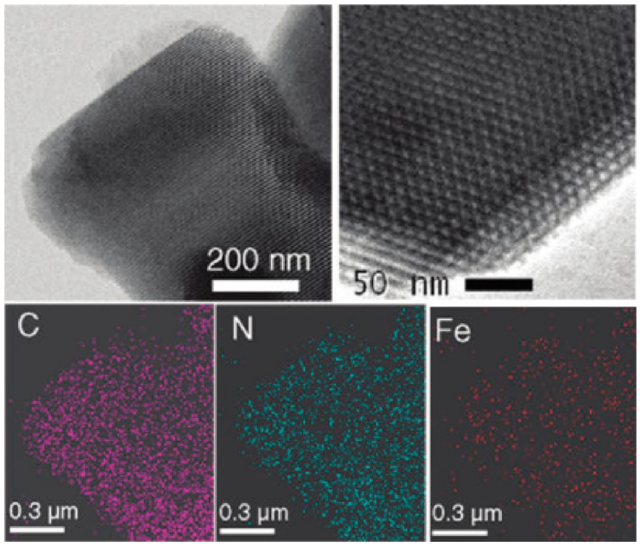

Figure 3. Typical TEM images of Fe-g-C_3N_4/SBA-15 and the corresponding elemental mapping images for C, N, and Fe.[26] Reprinted with permission from ref 26. Copyright 2009 American Chemical Society Publishing.

phenol using H_2O_2 as oxidant, because of the increase in surface area and possibly the change in surface morphology.

Another strategy, that is more effective in improving the surface area, is to synthesize a material with porous structure using a template method, as illustrated in Figure 4A, which can

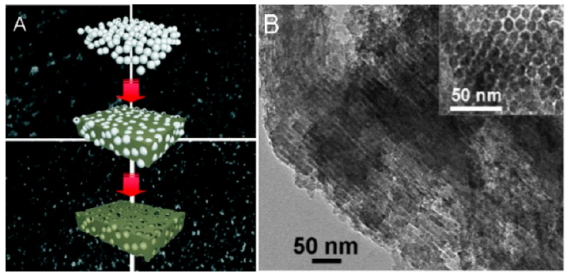

Figure 4. (A) Sketch for the preparation of porous g-C_3N_4 using a hard template. Reprinted with permission from ref 28. Copyright 2008 American Chemical Society. (B) TEM image of g-C_3N_4 replicated from SBA-15. Reprinted with permission from ref 29. Copyright 2009 John Wiley & Sons.

be seen as the result of removing the support from a g-C_3N_4-support composite. Indeed, it is reported in the literature that porous g-C_3N_4 with an improved surface area can be prepared using Ludox HS40 Silica as a template and, more interestingly, the surface area and total pore volume of g-C_3N_4 can be controlled by simply adjusting the mass ratio of precursor to silica template.[14] g-C_3N_4 materials with various structures and surface morphologies can be fabricated due to their polymeric properties, when appropriate templates are used.[28,30] For instance, Jun et al. report that 2D g-C_3N_4 can be replicated from ordered mesoporous SBA-15, as shown in Figure 4B.[29]

Porous g-C_3N_4 can also be synthesized using surfactants (e.g., Triton X-100, P123, Brij 58) or ionic liquids as soft templates through a self-polymerization reaction.[31,32] However, the final product can be contaminated with residual carbon coming from the template polymers, which can easily be identified by the naked eye, as the obtained g-C_3N_4 is black, instead of yellow. The preparation of porous g-C_3N_4 with structured (like SBA-15) and soft templates are illustrated in a previous review article.[19] The successful fabrication of g-C_3N_4 using different templates makes possible to synthesize materials with the desired porous structures and surface morphologies, for specific uses.

Oxygen-containing materials can also be used as precursors to produce g-C_3N_4. Dong et al. report that heating urea in a muffle furnace in the range of 450−600 °C for 2 h, with a heating rate of 15 °C min^{-1}, results in the formation of g-C_3N_4.[33] In particular, the authors state that the heating temperature significantly affects the thickness and surface area of the resulting material, as shown in Figure 5. The layer

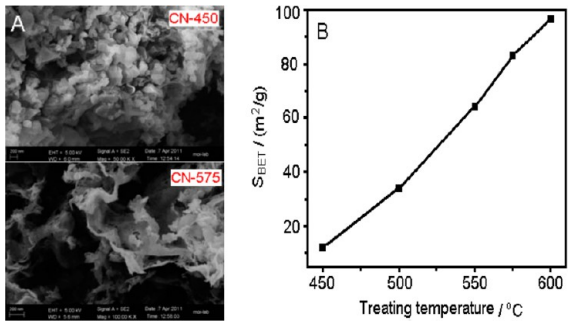

Figure 5. (A) TEM images of g-C_3N_4 synthesized at 450 and 575 °C using urea as precursor. (B) Dependence of the surface area of g-C_3N_4 on the treating temperature. Reprinted with permission from ref 33. Copyright 2011 Royal Society of Chemistry.

thickness decreases from 30 nm, for g-C_3N_4 synthesized at 450 °C (CN-450), to 20 nm, for the material synthesized at 575 °C (CN-575). Accordingly, the surface area increases from 12 m^2/g for CN-450 to 83 m^2/g for CN-575. This is interesting, as high-surface-area g-C_3N_4 (up to ca. 97 m^2/g) can be obtained by direct polycondensation without the use of a template. However, the formation mechanism is not yet clearly understood.

Similarly to what is observed for cyanamide in Figure 2B, Zou et al. claim that the temperature for g-C_3N_4 formation, using urea as precursor, can be lowered to 300 °C when the synthesis is conducted on OH-rich mesoporous TiO_2 spheres.[34] They believe that the low temperature needed is due to the presence of −OH groups, and a mechanism regarding the role of these groups in the synthesis process is proposed, as depicted in Scheme 1, where titanol groups (Ti−OH) are used to attack the carbonyl of isocyanic acid (eq 2), to form Ti-NH_2 groups, which subsequently react with cyanic acid to generate cyanamide (eq 3) and finally yield g-C_3N_4 (eq 4).

Besides the above-mentioned methods, there are many other procedures described for the synthesis of g-C_3N_4 with different surface morphologies and textural structures.[35−37] Dai et al. report that g-C_3N_4 submicrospheres can be synthesized by a microwave method and that the prepared g-C_3N_4 has a surface area of up to 89.1 m^2/g.[35] There are several reviews[5,19,38−40] that summarize the methods for the preparation of g-C_3N_4, with controllable morphology and structure. Those procedures are not mentioned in this work in order to avoid repetitions. Interested readers are referred to those publications.[5,19,38−40]

Scheme 1. Proposed Mechanism for the Formation of g-C_3N_4 Starting from Urea and Conducted on an OH-Rich TiO_2 Support[a]

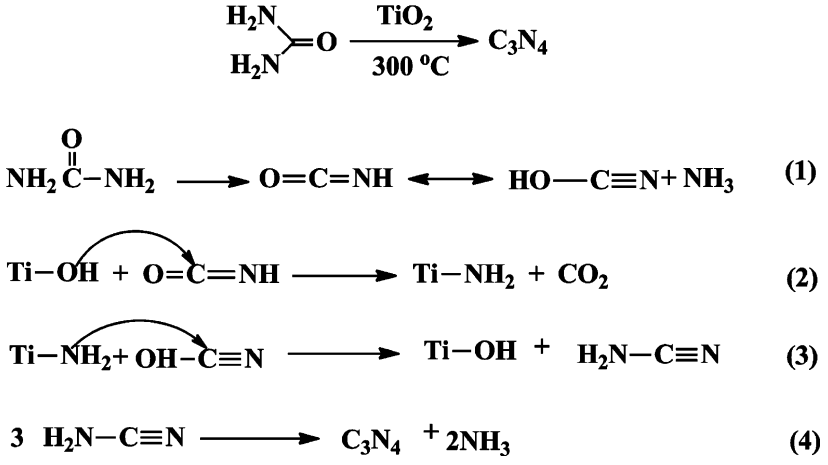

[a]Reprinted with permission from ref 34. Copyright 2011 Royal Society of Chemistry.

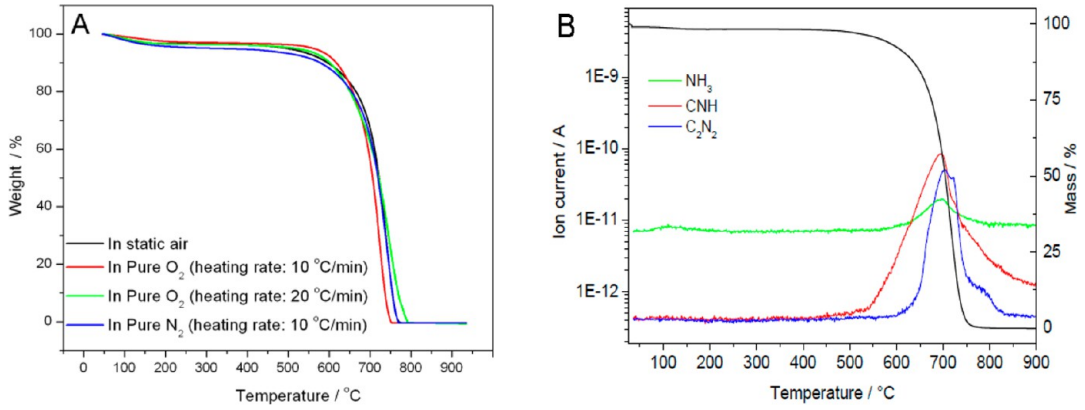

Figure 6. (A) TGA curves for g-C_3N_4 conducted in different atmospheres. Reprinted with permission from ref 7. Copyright 2012 Elsevier Publishing. (B) TGA-MS spectra of g-C_3N_4 obtained at the temperature of 530 °C. Reprinted with permission from ref 41. Copyright 2009 Universitätsbibliothek Potsdam & MPI of Colloids and Interfaces.

3. PHYSICOCHEMICAL PROPERTIES

Polymeric materials normally show low thermal stability and are readily oxidized (gasified) in oxidizing atmosphere, which makes them unsuitable as practical catalysts, especially for reactions conducted at high temperature ranges. In order to confirm that g-C_3N_4 has sufficient thermal stability for catalytic use, thermal gravimetric analysis (TGA) measurements need to be performed, as they reflect the thermal behavior of materials and provide direct evidence of which temperature ranges the materials can endure.

Figure 6A depicts the TGA curves of g-C_3N_4 obtained with different conditions, showing that the material is stable up to 600 °C, either in N_2, O_2 or air atmosphere, and that the TGA curves obtained are similar.[7] This suggests that g-C_3N_4 can endure high temperatures, even in oxidizing atmosphere, and the weight loss at above 600 °C is not due to the oxidation by O_2 (to form oxides such as CO or CO_2), but to the direct thermal decomposition of g-C_3N_4 itself. Combined TGA-MS results confirm that the decomposition products contain mainly CNH, NH_3 and C_2N_2 species, and that no oxide product is detected, as shown in Figure 6B.[41] This shows that g-C_3N_4 is inert in oxygen atmosphere, otherwise the TGA profiles would be different when N_2 and O_2 are used, and oxidized products would be formed. The high thermal stability demonstrates that g-C_3N_4 can work for reactions conducted in oxidative atmosphere and at high temperatures. Due to its chemical inertness to molecular oxygen, it is expected that g-C_3N_4 can show interesting results in catalysis, unlike traditional inorganic materials that are reactive to molecular oxygen.

g-C_3N_4 also shows good chemical stability in a variety of conventional solvents, including water, alcohols, dimethylformamide, tetrahydrofuran, diethyl ether and toluene, which makes it an excellent material, not only for gas-phase reactions conducted at elevated temperatures (as mentioned above), but also for liquid-phase reactions, carried out in various solvents. It is reported that no essential change in the IR spectra is observed for g-C_3N_4 after it is soaked in the above solutions for up to 30 days, confirming its excellent stability and durability.[18] However, exceptions are reported, when the material is treated in molten alkali metal hydroxides and concentrated acids.[42]

As demonstrated above, the replacement of C by N in the six-membered C−N−C rings produces surface basic groups on the g-C_3N_4 surface, which facilitates its use as a base catalyst. The importance of the surface basicity of g-C_3N_4 is demonstrated in several reactions, including C−C coupling,[43] α−C-H activation[44] and NO decomposition.[7] The surface basicity of g-C_3N_4 can be identified and evaluated by temperature-programmed desorption of CO_2 (CO_2-TPD),

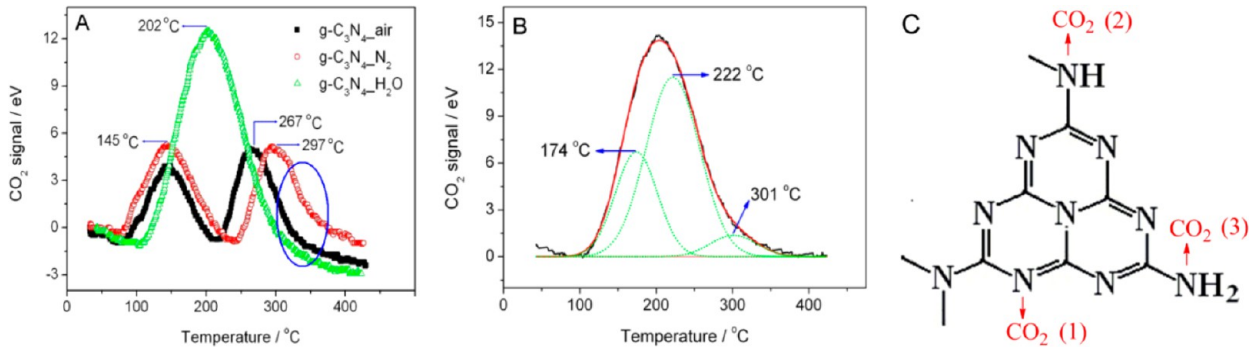

Figure 7. (A) CO_2-TPD profiles of g-C_3N_4 synthesized under different conditions; (B) peak deconvolution for the CO_2-TPD profile of g-C_3N_4_H_2O; (C) Possible basic sites used for CO_2 adsorption on g-C_3N_4.

which is a powerful technique in measuring the surface basicity of materials. In several recent works, it is shown that covalent triazine frameworks (CTFs), which are a kind of carbon nitrides, exhibit good surface basicity and show excellent performances for the synthesis of cyclic and linear carbonates from CO_2 and epoxides, as well as for dye removal by adsorption.[45,46]

Figure 7A depicts the CO_2-TPD profiles of g-C_3N_4 synthesized under different conditions, which show a large amount of surface basic groups. It is known that there are three types of surface basic sites in which CO_2 can be adsorbed on, namely: "≡N" in the C−N−C six-membered rings, and "═NH" and "−NH_2" groups on the surface edges, as shown in Figure 7C, which result in three deconvoluted CO_2 desorption peaks in the CO_2-TPD profile. The former two desorption peaks are clearly observed, whereas the latter appears above 300 °C and is overlapped, as shown in the TPD profile.

Although the XRD patterns show no change in the bulk structure, it was found that the surface basicity is significantly affected if g-C_3N_4 is synthesized in different atmospheres. The sample prepared by thermal condensation of cyanamide, in nitrogen atmosphere, at 550 °C for 4 h (g-C_3N_4_N_2), shows two desorption peaks at 145 and 297 °C, which become closer when the sample is synthesized in air atmosphere (g-C_3N_4_air). Moreover, only one CO_2 desorption peak is found for g-C_3N_4_H_2O, prepared by first dissolving the precursor cyanamide in aqueous solution and subsequently treated in air atmosphere. This desorption profile can be deconvoluted into three peaks, in terms of the basic sites analyzed above, as shown in Figure 7B, and the temperature difference for the former two desorption peaks is closer. The shift in the desorption temperature suggests that the surface basic intensity of g-C_3N_4 is changed, which might be caused by the vapors in the environment, as the percentage of vapors found in the atmosphere increases from g-C_3N_4_N_2 to g-C_3N_4_air and further to g-C_3N_4_H_2O. It is reported that the vapors in the heating atmosphere facilitate the release of NH_3 from nitrogen containing carbonaceous materials, and change the surface basicity of material,[47,48] supporting the above results.

Modifications or functionalizations of g-C_3N_4 are often carried out to widen its applications and discover its essential properties. Both in situ modification and postfunctionalization are possible. g-C_3N_4 can be in situ doped with boron,[44] fluorine,[49] sulfur,[50] phosphor[51] or protonated with HCl.[42] That is well-documented and summarized in several reviews.[4,18] Such modifications enhance the properties of the material and improve its applications. For example, the doping with phosphor can improve the electric conductivity by 4 orders of magnitude and photocurrent generation by 5 orders of magnitude, compared to the pure g-C_3N_4.[51] Many other interesting physicochemical properties of g-C_3N_4 are introduced and documented in other works.[4,18−21] For space limitations and to avoid repetition they are not detailed in this review. Interested readers are referred to those publications.[4,18−21] It should be noted, however, that such modifications or functionalizations are very useful for changing the surface properties of g-C_3N_4, and are especially important concerning the optimization of its catalytic performance.

4. MULTIFUNCTIONAL APPLICATIONS IN CATALYSIS

The applications of g-C_3N_4 in catalysis have been extensively investigated in recent years, and it is now established that g-C_3N_4 is a good catalyst for a wide variety of reactions. In order to differentiate and avoid overlapping the contents of previous works, in this review, the applications of g-C_3N_4 in heterogeneous catalysis are referred from three different aspects, and the reasons for the use of this material in such applications is given. The first point is the use of g-C_3N_4 as a metal-free catalyst for catalytic reactions (namely NO decomposition); the second is its use as a reference material, to differentiate the oxygen activation sites in oxidation reactions conducted on supported catalysts; and the third is its application as a high surface support with a large amount of functional groups, ideal to prepare small and stable metal nanoparticles (NPs). Also, the application of g-C_3N_4 in photocatalysis, one of the most current research topics worldwide, is described, based on the achievements mentioned in the literature. We expect that this work will inform the reader about the multifunctional properties of this exciting material and that will stimulate research to find new applications in heterogeneous catalysis or other fields in the future.

4.1. As a Metal-Free Catalyst for NO Decomposition.

Nitrogen monoxide (NO) is a hazardous pollutant that causes environmental problems, such as acid rain and urban smog, and its removal is a challenging task nowadays.[52] Direct decomposition of NO into N_2 and O_2 (2 NO → N_2 + O_2) is an ideal route for NO removal, as no reductant is needed and the products are the nontoxic N_2 and O_2. However, this reaction route is not yet carried out in industry since current inorganic catalysts encounter many problems when operating in real conditions. Another problem is that gaseous oxygen in the reacting atmosphere has negative effects on the reaction, namely: (1) it suppresses the desorption of atomic oxygen (formed in NO dissociation) from the active sites, making their

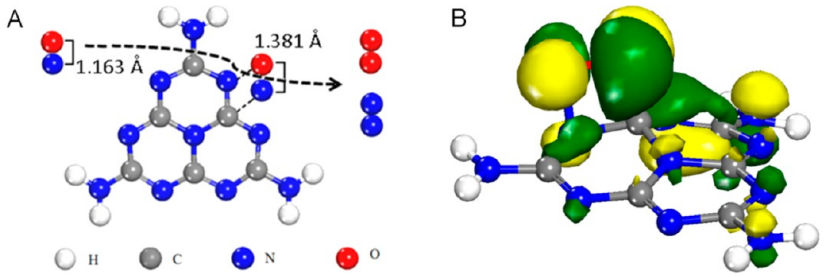

Figure 8. (A) Theoretical simulation of NO decomposition on g-C_3N_4 by density functional theory (DFT) calculation; (B) theoretic model for calculating the Mulliken charge distribution of NO before and after adsorption on g-C_3N_4. Reprinted with permission from ref 7. Copyright 2010 Royal Society of Chemistry.

regeneration difficult and thus poisoning the catalyst; (2) it competes with NO on the surface oxygen defects (active sites) during the adsorption process, preventing NO adsorption and activation on the catalyst surface and thus decreasing the activity.[53,54]

From the molecular orbital diagram of the NO molecule, $(\sigma_{1s})^2(\sigma_{1s}^*)^2(\sigma_{2s})^2(\sigma_{2s}^*)^2(\sigma_{2p})^2(\pi_{2p})^4(\pi_{2p}^*)^1$, it is known that the bond order of N−O is 2.5, and can be lowered to 2.0, if NO gains an electron in the (π_{2p}^*) energy band, which favors the rupture of the N−O bond. Hence, an ideal NO decomposition catalyst should have weak interactions or be inert to oxygen, in order to avoid the negative effects caused by this gas, and have electron-rich properties, so that it can donate electrons to NO and thus decrease the order of the N−O bond.

g-C_3N_4 has strong resistance to oxygen and electron-rich properties (surface basic sites), being a suitable catalyst for NO decomposition. In addition, the polar C−N−C groups of g-C_3N_4 can also provide ideal adsorption sites for NO (that is a polar molecule). In order to verify the applicability of g-C_3N_4 to NO decomposition, theoretical simulations based on density functional theory (DFT) calculations were attempted, showing that the N−O bond length can be elongated from 1.163 to 1.381 Å when NO is parallelly adsorbed on g-C_3N_4, as shown in Figure 8A, confirming that g-C_3N_4 is a suitable catalyst for NO dissociation.[7]

To explain NO dissociation on g-C_3N_4, we calculated the Mulliken charge distributions of NO before and after adsorption on the material, as depicted in Figure 8B and Table 1, showing that the values varies from 0 for the free NO molecule to −0.271 when it is adsorbed, and the change in q_O is more negative than that in q_N.[7] This shows that electrons are transferred from g-C_3N_4 to the NO molecule, and that the O atom of NO is connected to the basic sites of g-C_3N_4. These results explain why NO can be dissociated on g-C_3N_4 and suggest that g-C_3N_4 can catalyze NO decomposition (at least in theory).

Table 1. Mulliken Charge Distribution of Different Atoms before and after the Adsorption of NO on g-C_3N_4[a] [7]

	q_N	q_O	q_{NO}	q_{Csub}	q_{Nsub}
after adsorption	−0.091	−0.180	−0.271	0.375	−0.232
before adsorption	0.040	−0.040	0.000	0.450	−0.379

[a] q_N: The Mulliken charge of N atom of NO; q_O: The Mulliken charge of O atom of NO; q_{NO}: The Mulliken charge of NO; q_{Csub}: The Mulliken charge of C atom of C_3N_4; q_{Nsub}: The Mulliken charge of N atom of C_3N_4

The suitability of g-C_3N_4 to catalyze NO decomposition is confirmed by the experimental results shown in Table 2, which demonstrate that g-C_3N_4 is active for NO decomposition at temperatures above 400 °C, and that the activity increases with temperature, in accordance with the DFT calculations. The activity can be further increased when metal ions (e.g., Na^+, Zn^{2+}, Au, etc.) are incorporated into the framework.

Table 2. NO Conversion over Several g-C_3N_4-Based Catalysts at Different Temperatures.[7]

	NO conversion (%) at different temperatures			
catalyst	400 °C	450 °C	475 °C	500 °C
g-C_3N_4	0.14	3.46	5.03	15.06
g-C_3N_4[a]	2.14	18.58	33.33	46.25
Zn-g-C_3N_4	10.83	32.37	48.31	69.40
Pt-g-C_3N_4	7.46	19.92	35.65	49.61
Au-g-C_3N_4	26.88	23.01	26.59	41.05

[a] g-C_3N_4 synthesized in basic medium before calcination

Very interestingly, the incorporation of zinc (i.e., Zn-g-C_3N_4) leads to similar or even better NO decomposition activities, compared to noble metals (e.g., Pt-g-C_3N_4). Considering that Zn is inactive for NO decomposition, while Pt is active, the comparable activities observed for the Zn- and Pt- incorporated samples suggest that the metal in g-C_3N_4 is not the active site. This suggests that the surface basic sites of g-C_3N_4 are responsible for the activity, as indicated in DFT simulations (cf. Figure 8A). The excellent behavior of g-C_3N_4 for base reactions is well-documented in a recent paper by Li et al., based on a Schottky effect.[20] This result opens a new panorama to design low-cost (noble metal free), green, and environmentally friendly catalysts for NO decomposition.

It is worth to point out that since g-C_3N_4 has a strong resistance to oxygen, the NO decomposition reaction thus can be conducted in the presence of this gas, without the negative effects observed for inorganic catalysts. This makes g-C_3N_4 a very attractive catalyst, compared to others reported in the literature, and reinforces its potential role in NO decomposition in the future.

4.2. As a Reference Material to Differentiate O_2 Activation Site. Catalytic oxidation is one of the most important reactions in industry and our daily life. Molecular oxygen is the preferred oxidant due to its easy availability, low cost and nontoxicity. As O_2 molecule is not very active, it should be activated and dissociated into atomic oxygen before participating in the reaction.[55] The pathway for oxygen activation is still under discussion, especially for reactions carried out on supported catalysts. Schubert et al. suggest three

possible pathways for oxygen activation on supported catalysts: one takes place on supported metal particles such as gold; the other on the supports such as Fe_3O_4; and the third on the interface of the support and the metal particles, as shown in Figure 9.[56] Accordingly, the supports are classified into "active" and "inert" types. For example, MgO is considered as an "inert" support and the oxygen activation takes place mainly on the Au particles, for $CO+O_2$ reaction on Au/MgO catalysts. However, other authors state that the CO oxidation activity is proportional to the amount of "F centers" in the MgO support of Au/MgO catalyst.[57] Although much effort was made to clarify the oxygen activation pathway, no clear conclusion was reached up to now, being the pathway of oxygen activation still unclear. However, the number of articles dealing with the adsorption and activation of molecular oxygen on oxide supports is increasing.[58−63]

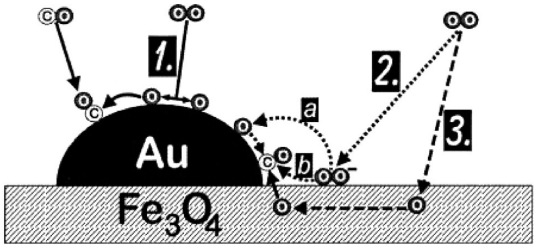

Figure 9. Possible activation routes for molecular oxygen for CO oxidation on Au/Fe_3O_4 catalysts. Reprinted with permission from ref 56. Copyright 2001 Elsevier Publishing.

An effective and simple way for clarifying the oxygen activation pathway over supported catalysts is the use of an oxygen-free and oxygen-inert support as a reference, so that the activation of molecular oxygen, if happening, can only proceed on the metal NPs. However, oxygen-free materials (e.g., carbon or metal nitride) are usually unstable in the presence of oxygen, and are easily gasified or oxidized at high temperatures, making them unsuitable for catalytic oxidations. Hence, g-C_3N_4 is useful as it is not only an oxygen-free and oxygen-inert material but also has high thermal stability even in oxygen atmosphere (cf. Figure 6). Therefore, it can be inferred that if g-C_3N_4 supported metal catalysts are active for oxidation reaction using oxygen as oxidant, the oxygen must be activated on the metal sites. Thus, this principle can be used to test if the activation of molecular oxygen occurs on metal sites or on a support, by replacing that support by g-C_3N_4, and comparing the obtained activities.

Figure 10A compares the catalytic performances of gold NPs supported on activated carbon (Au/AC) and g-C_3N_4 (Au/g-C_3N_4) for the selective oxidation of benzyl alcohol using molecular oxygen as oxidant.[64] The Au/AC catalyst shows 90.8% conversion for benzyl alcohol for reaction time of 3 h, while that obtained from the Au/g-C_3N_4 catalyst is only 5.7% even after 5 h. Considering that the adsorption and activation of benzyl alcohol on Au NPs readily occur,[65,66] the low activity observed for Au/g-C_3N_4 suggests that the molecular oxygen is not being activated. That is, the Au NPs, as well as the g-C_3N_4, cannot activate the molecular oxygen in the reaction. Consequently, it is inferred that the molecular oxygen is only activated on the AC support, when Au/AC is used as catalyst. Similar results were also observed for $CO+O_2$ reaction.[64]

Catalytic performances were investigated for benzyl alcohol oxidation reaction using Au NPs supported on AC with different amounts of surface oxygen functional groups (SOFG), in order to investigate how molecular oxygen is activated on this support. The results show that the conversion of benzyl alcohol depends intimately on the amount of SOFG, as seen in Figure 10B,[64] suggesting that the oxygen activation proceeds through the SOFG of AC. This is also supported by FT-IR and UV−vis measurements.[67] It is therefore explained why Au NPs supported on g-C_3N_4 (i.e., Au/g-C_3N_4) show negligible activity, as g-C_3N_4 has no SOFG and hence no oxygen activation sites.

An interesting work regarding the catalytic performances of Au and Pt NPs supported on carbon nitrides−silica composites (CNx/SBA-15) for $CO+O_2$ reaction was recently reported.[68] Although both metals have small particle size (<5 nm), they show different catalytic performances for CO oxidation. The gold catalyst (Au/CNx/SBA-15) shows negligible activity, while the platinum catalyst (Pt/CNx/SBA-15) is quite active for the reaction, as seen in Figure 11. This is explained by the fact that Au NPs are in the metallic state and cannot provide sites for oxygen activation, whereas Pt NPs are partially oxidized thus having the ability to activate molecular oxygen.[68] This again shows the need of using g-C_3N_4 as a reference material, in order to clarify the oxygen activation pathway on supported catalysts. The inertness of Au NPs to molecular oxygen is reported by several other authors. One example is the work of Lambert et al., who claim that Au NPs supported on boron nitride (Au/BN), an oxygen-free material, cannot

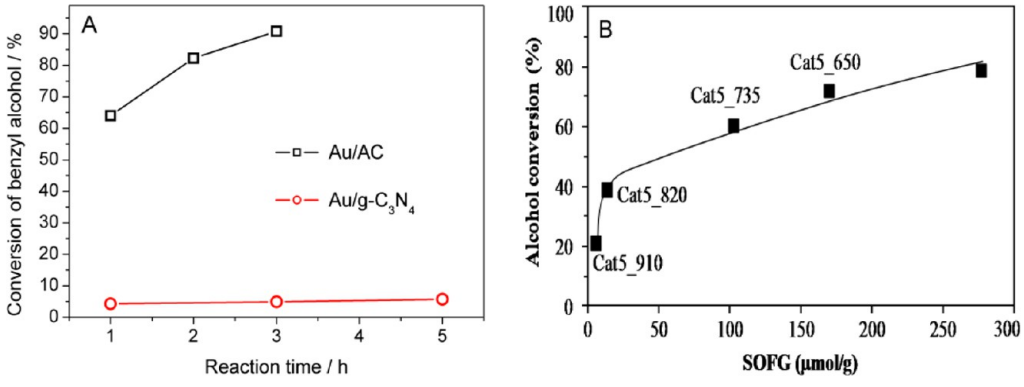

Figure 10. (A) Conversion of benzyl alcohol measured on Au/AC and Au/g-C_3N_4. (B) Conversion of benzyl alcohol obtained on the catalysts Cat5_T, versus the amount of surface oxygen functional groups (SOFG) of the corresponding carbon supports (AC5_T). Reprinted with permission from ref 64. Copyright 2010 Elsevier.

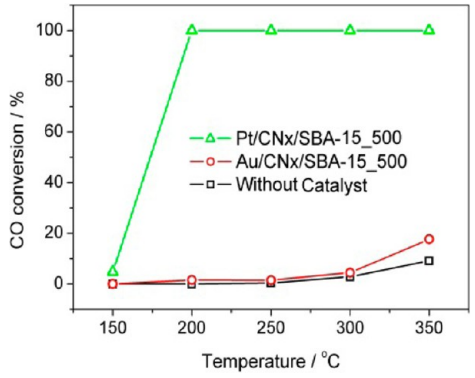

Figure 11. CO conversion on Pt/CNx/SBA-15_500, Au/CNx/SBA-15_500, and without catalyst (blank test). Reprinted with permission from ref 68. Copyright 2014 John Wiley & Sons.

activate molecular oxygen and show no activity for CO oxidation for particle sizes above 2 nm.[69]

The principle of using g-C_3N_4 as a reference material to clarify the sites of oxygen activation on supported catalysts can be simply expressed by Scheme 2. If an active supported catalyst (e.g., Au/AC) loses its activity for oxidation after the support (AC) is replaced by g-C_3N_4, then oxygen activation does not occur on the metal sites (Au), but on the support (AC). However, if high oxidation activity is obtained for metal NPs (e.g., Au, Pt) supported on g-C_3N_4, it can be inferred that oxygen activation occurs on the metal (e.g., Pt) sites, otherwise the metal (e.g., Au) would not be able to activate molecular oxygen. This principle offers a facile way to differentiate the sites of O_2 activation on a supported catalyst.

4.3. As a Functional Material to Prepare Small and Stable Nanoparticles. Nanocatalysis is one of the most exciting subfields of nanoscience, which aims to prepare nanoscale catalysts to control the activity and selectivity of reactions.[70−72] It is generally accepted that catalysts prepared in the nanoscale show enhanced catalytic performances than those in bulk, due to the quantum confinement effects.[73] However, ensuring the stability of the supported NPs and preventing their agglomeration and ripening in the reaction is still a complicated task.[74−76] The preparation of nanoscale catalysts with high thermal stability is of interest, as it can not only broaden their applications, but also increase their durability.

A good support should not only have high surface area to disperse the NPs, but also strong affinity for them, preventing their movement or leaching during the reaction. Nevertheless, the majority of the reported inorganic supports, such as AC, TiO_2, SBA-15, show deficiencies in these aspects.[75,77−79] For example, SBA-15 has ordered mesoporous structure and high surface area, but shows a relatively inert surface, not being good for grafting metal NPs.[75] In this respect, a number of works report the use of organic groups, such as amine or thiol, to activate or functionalize the surface before being impregnated with the metal ions. However, such functional groups can be problematic if the final catalyst is to be used at high temperatures, as they can be thermally cleaved and release high energy,[75] which would lead to agglomeration or leaching of the NPs during the reaction.

A recent report proved CTF to be a better support for palladium catalysts, for alcohol oxidation, compared to AC, due to its high surface area and, especially, its basic surface properties.[77,80,81] The Pd/CTF catalyst shows not only better activity but also stronger resistance to aggregation than the Pd/AC analogue. However, the low thermal stability of CTF makes such catalysts hard to be used in reactions carried out at high temperatures. Therefore, the use of g-C_3N_4 as support for metal NPs can have advantages, as it also has basic surface sites and is stable up to 600 °C, even in air atmosphere.

It was suggested to prepare g-C_3N_4 as a film, on a high-surface-area material, in order to improve its surface area and better used it as a catalyst or a support.[26] The film can retain the intrinsic properties of the material, even after being impregnated on a support, because g-C_3N_4 is a polymeric material and generally does not react with inert supports, such as SBA-15,[29] to form new compounds. Moreover, the thickness of the layer can be controlled by simply increasing the polycondensation temperature or extending the polycondensation time, as illustrated in Figure 12, which shows polymeric carbon nitrides (CNx) supported on SBA-15.[68]

The use of CNx in the preparation of metal NPs can be exemplified by the CNx/SBA-15_T composite, treated at different temperatures ranging from 300 to 500 °C.[29] Although the degree of condensation differs because of the different temperatures used, the resulting samples have graphitic structure and surface basic sites, and the obtained conclusions can be applied to g-C_3N_4, normally obtained at 550 °C.

Figure 13 shows Au and Pt NPs supported on SBA-15 and CNx/SBA-15_500 (Au/SBA-15 vs Au/CNx/SBA-15_500 and Pt/SBA-15 vs Pt/CNx/SBA-15_500). Both Au and Pt NPs are severely aggregated and confined to a small area when

Scheme 2. Principle for Identification of the Oxygen Activation Site Using g-C_3N_4 as a Reference Material

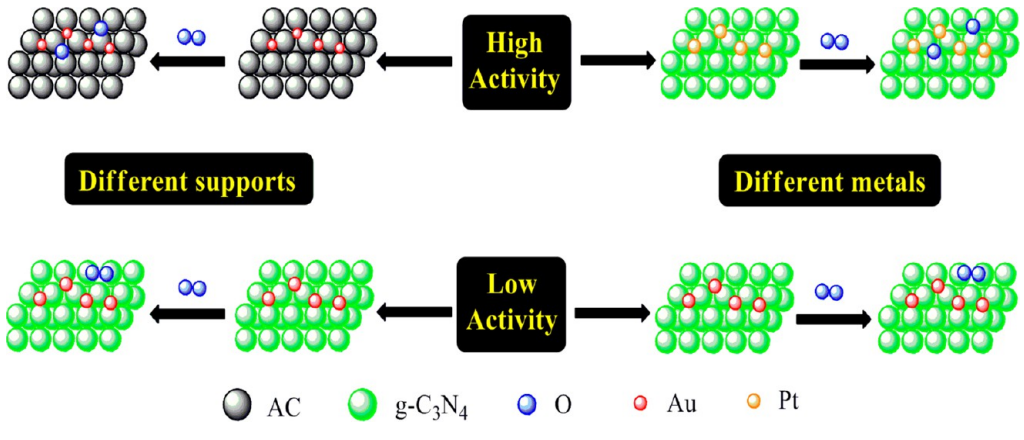

dx.doi.org/10.1021/am502925j | ACS Appl. Mater. Interfaces 2014, 6, 16449−16465

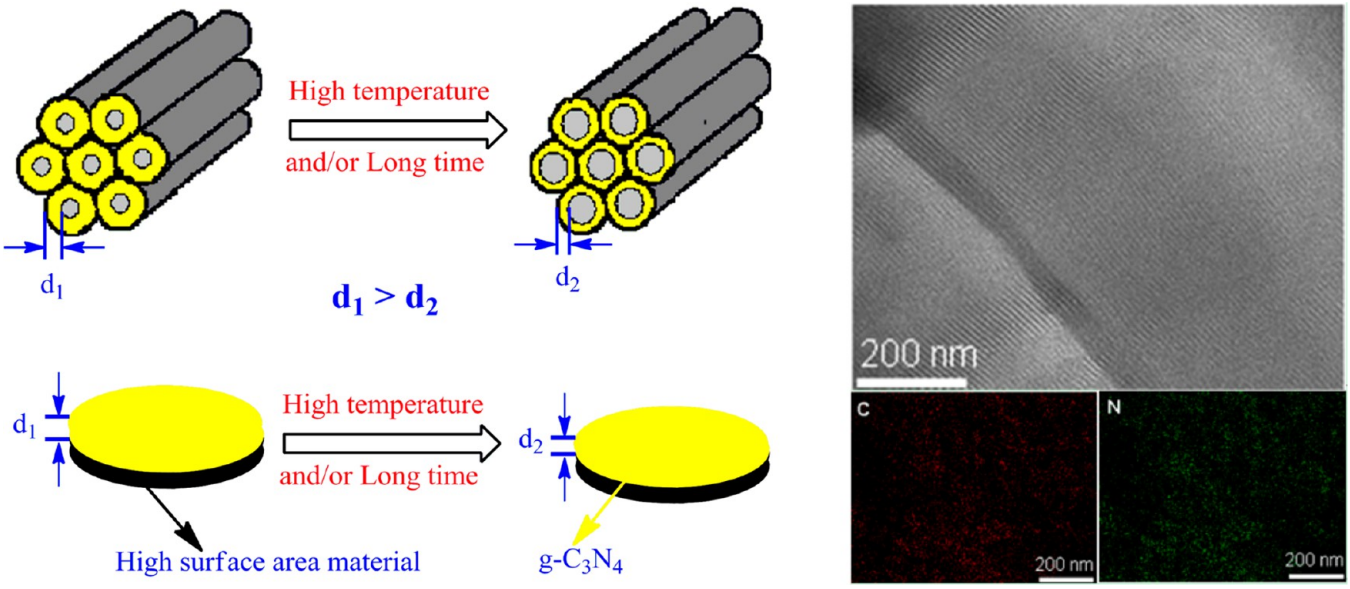

Figure 12. Controlling the thickness of g-C_3N_4 supported on a high-surface-area material by changing the polycondensation temperature and/or time (left); TEM image and respective element mapping of CNx/SBA-15_500 (right). Reprinted with permission from ref 68. Copyright 2014 John Wiley & Sons.

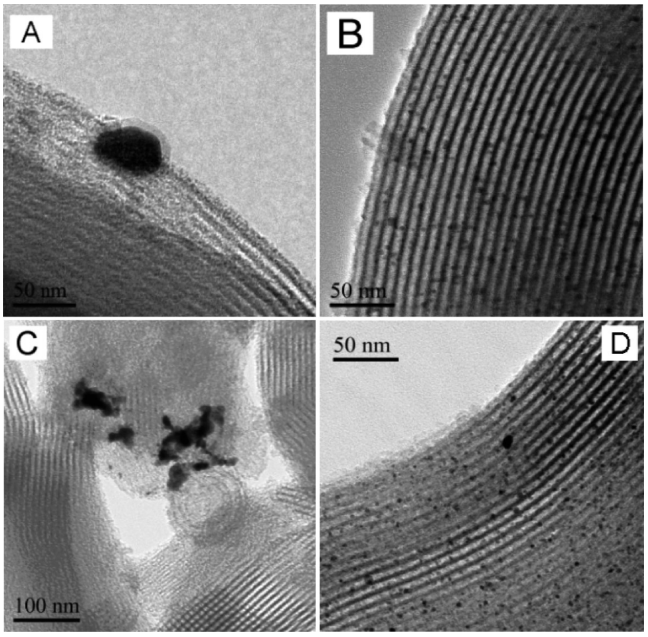

Figure 13. TEM images of (A) Au/SBA-15, (B) Au/g-C_3N_4/SBA-15_500, (C) Pt/SBA-15, and (D) Pt/g-C_3N_4/SBA-15_500. Reprinted with permission from ref 68. Copyright 2014 John Wiley & Sons.

deposited directly on the SBA-15 support. It is hard to obtain individual particles supported on SBA-15, but they can be highly dispersed on CNx/SBA-15_500 and have small sizes. The improvement in dispersion and the decrease in particle size shows that the presence of CNx indeed facilitates the formation of small and stable Au/Pt NPs. Similar results can be obtained using SBA-16 instead of SBA-15, implying that this change is indeed caused by CNx and not by SBA-15.[68]

Interestingly, it was found that the particle size of metal NPs can be controlled, using supports with different loading or thickness of the CNx layer. The particle size of Au NPs supported on CNx/SBA-15_T (where *T* is the treatment temperature of CNx/SBA-15), follows the sequence: Au/CNx/SBA-15_300 < Au/CNx/SBA-15_400 < Au/CNx/SBA-15_500 (Figure 14), which is the inverse order of the loadings

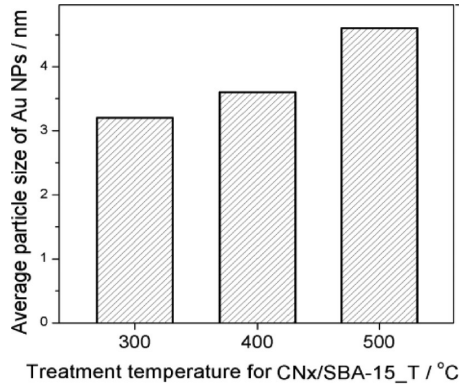

Figure 14. Dependence of particle size of Au NPs on the thickness of CNx or the treatment temperature of CNx/SBA-15_T. Reprinted with permission from ref 68. Copyright 2014 John Wiley & Sons.

or thickness of CNx on SBA-15.[68] Hence, the particle size of Au NPs can be controlled by adjusting the loading or the thermal treatment temperature of CNx. This implies that CNx is the adsorption site of Au and Pt NPs. Therefore, the CNx/SBA-15_300, which has the highest CNx loading, provides the largest amount of adsorption sites for Au and Pt NPs, improving the dispersion and decreasing the particle size.

Traditional functional groups like amine or thiol, which are used as intermediate species to graft metal NPs, decompose during the catalyst calcination process, usually conducted above 300 °C; thus the NPs interact directly with the support in the final product. However, g-C_3N_4 has high thermal stability (cf. Figure 6), being present in the final product. Thus, the NPs interact with g-C_3N_4 and not with the support (e.g., SBA-15), so they stay on the adsorption sites of g-C_3N_4, and are stable on the surface, even at high temperatures (below the decomposition point of g-C_3N_4). TGA profiles show that the weight

dx.doi.org/10.1021/am502925j | ACS Appl. Mater. Interfaces 2014, 6, 16449−16465

loss in CNx/SBA-15_500 and Au/CNx/SBA-15_500 is almost the same, supporting this assumption.

Besides being coated on a high-surface-area material, g-C_3N_4 itself can be used to support small and stable metal NPs, if synthesized with a porous structure.[82−86] Wang et al. report the preparation of Pd NPs with particle size of ca. 3 nm on a mesoporous g-C_3N_4 (i.e., Pd@mpg-C_3N_4) that show high stability and activity either in hydrogenation or photocatalytic reactions.[82,86] Li et al. report that mesoporous g-C_3N_4 nanorods are multifunctional supports in the preparation of ultrafine metal NPs (with sizes as low as 2 nm for Pt, Au and Pd) for hydrogen generation and nitrophenol reduction.[87] These findings confirm that g-C_3N_4 is the adsorption site of metal NPs and has good ability to disperse and stabilize the metal NPs on its surface.

To illustrate the advantages of using g-C_3N_4 in the preparation of metal NPs for catalysis, the performances of Pt NPs supported on SBA-15 and CNx/SBA-15_500 for catalyzing CO + O_2 reaction are compared in Figure 15.[68]

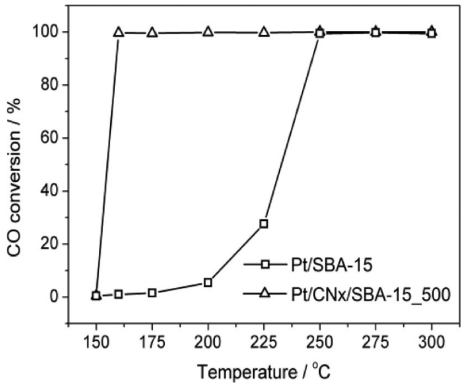

Figure 15. CO conversion using Pt/SBA-15 and Pt/g-C_3N_4/SBA-15 as catalysts. Reprinted with permission from ref 68. Copyright 2014 John Wiley & Sons.

Obviously, Pt/g-C_3N_4/SBA-15 shows enhanced CO oxidation activity compared to Pt/SBA-15. This is explained by the high dispersion and small particle size of Pt NPs in the former, since CNx cannot activate molecular oxygen and give a small contribution to the reaction. Furthermore, the Pt NPs are stable during the reaction and only a small increase of 0.6 nm in the particle size is observed after three catalytic cycles.[68] This indicates that the carbon nitrides, although not contributing directly to the reaction, improve the catalytic performance of metal NPs, by decreasing their particle size. Carbon nitrides also prolong the catalysts lifetime through stabilization of the NPs during the reaction.

4.4. As a Metal-Free Catalyst for Photocatalysis. Compared to the conventional thermal catalysis, semiconductor photocatalysis is another efficient technology which uses the photons energy to activate the catalyst and, subsequently, to catalyze the reaction. The solar energy is an endless and environmentally friendly source, which makes photocatalysis an attractive technology for solving environmental and energy problems, such as water contaminants degradation,[88−90] water splitting,[91−93] CO_2 reduction,[94,95] and other chemical synthesis.[15,26,84,96] One challenging problem of this technology is to search for a suitable material that can efficiently harvest the photons, especially those from the visible light range. In fact, the search for visible light active photocatalysts, with rare earth and inexpensive elements, is a hot topic nowadays.

The applicability of polymeric g-C_3N_4 to photocatalysis was first reported by Wang et al. in 2009[97] and great achievements on the photocatalytic behavior and its reaction mechanism have been obtained thereafter. In contrast to the traditional inorganic metal catalysts, this metal-free material has high chemical stability and can be tailored as desired, due to its polymeric properties, making it a promising photocatalyst in aqueous solution. However, the photocatalytic efficiency of g-C_3N_4 is still limited due to the large optical band gap (2.7 eV, which corresponds to a utilization of solar energy at λ < 460 nm) and the fast recombination rate of photogenerated electron−hole pairs.[97,98]

Improving the use of visible-light energy and preventing the recombination of electron−hole pairs are two current concerns in the design of active photocatalysts. Moreover, conceiving a strategy to improve the photocatalytic activity of g-C_3N_4 is essential and of interest to readers working on photocatalysis. However, considering the many review articles published on the topic and in order to avoid overlapping of the contents reviewed, herein we refer mainly the efforts in improving the photocatalytic performances of g-C_3N_4 that deal with designing appropriate textural properties, doping, synthesizing inorganic−organic materials, and making composites with other semiconductor materials. Photocatalytic degradation of water contaminants, water-splitting, and chemicals synthesis (i.e., selective oxidation of benzene to phenol) are used as model reactions for discussion.

It is known that catalysis belongs to a class of surface reactions, and is sensitive to the surface structure and surface morphology of the catalyst, thus the fabrication of g-C_3N_4 with different textural structures (e.g., porous vs bulk) and surface morphologies is expected to affect the photocatalytic performances. On the one hand, materials with porous structure and high surface area can have more active sites for the adsorption and reaction of the reactants. On the other hand, samples with different morphologies are expected to show different surface properties and abilities to generate photons. As shown in the synthesis section, g-C_3N_4 can be produced with different textural structures and surface morphologies, using a template strategy or an appropriate precursor (e.g., urea), which can lead to the synthesis of g-C_3N_4 with improved photocatalytic performance. For example, Wang et al. report that mesoporous g-C_3N_4 with different textural structures (e.g., surface areas) can be obtained by modifying the silica/cyanamide mass ratio (silica is used as template and cyanamide as the precursor of g-C_3N_4), and surface areas can increase from 8 to 373 m^2/g when the mass ratio of silica/cyanamide ranges from 0 to 1.5. In particular, the efficiency of hydrogen production from the photochemical reduction of water can be improved by 8 times through the introduction of mesoporosity into g-C_3N_4, as shown in Table 3.[99] Other authors also found that g-C_3N_4, fabricated with nanoporous or mesoporous structure, can show a significant improvement in mineralizing organic pollutants in aqueous solution under visible light irradiation, because of their enlarged surface area and enhanced light-harvesting effect, which facilitate the photogeneration of active oxy-radicals in water.[100−102]

Doping is a traditional and effective strategy for improving photocatalytic efficiency due to its effectiveness in broadening the optical response range of semiconductor materials.[104] The doping of foreign elements onto the matrix structure can

Table 3. Textural Properties and Photocatalytic Activity of mpg-C_3N_4 for the Hydrogen Evolution Reaction with Visible Light[99]

entry	catalyst	surface area (m^2/g)	H_2 evolution rate (μmol/h)	TOF[a] × 100 (h^{-1})
1	mpg-$C_3N_{4/0.2}$	67	149	27
2	mpg-$C_3N_{4/0.5}$	126	142	26
3	mpg-$C_3N_{4/1.0}$	235	124	23
4	mpg-$C_3N_{4/1.5}$	373	69	13
5	g-C_3N_4	8	18	3
6[b]	g-C_3N_4	10	19	3

[a]Turnover frequency: $n_{(H2)}$ per $n_{(melem\ units)}$ per hour. [b]Subjected to the same NH_4HF_2 treatment as for the synthesis of mpg-C_3N_4.

change not only the textural structure, but also the chemical composition, atomic arrangement, physical dimensions (carrier limit) and electronic properties, and the band position of the photocatalyst, resulting in different abilities to capture the photons and separate the electron−hole pairs. The doping can be done in situ using the desired precursors (e.g., trithiocyanuric acid[105]) or using a postsynthesis strategy through treating a preformed g-C_3N_4 with the desired reagent (e.g., H_2O_2,[103] B_2O_3,[106] H_2S[50]), both leading to enhanced photocatalytic activities. Wang et al. report the synthesis of a sulfur doped carbon nitride (CNS) using amino-group free trithiocyanuric acid as precursor.[105] Those authors claim that the sulfur-mediated synthesis offers an effective approach to modify the texture, optical and electronic properties, and finally the photoactivity. In their studies, the best CNS sample (CNS650) shows an improvement in the H_2 evolution activity by a factor of 12, and the O_2 production activity by a factor of 5, compared to that of mpg-C_3N_4. That is, the water oxidation reaction (one of the half reactions of water splitting) can be achieved at a considerable rate without the aid of cofactors.

Chen et al. reported that O-doped g-C_3N_4 can be obtained by a facile H_2O_2 hydrothermal approach through postsynthesis.[103] The doping of oxygen to the framework of g-C_3N_4 extends the visible light response (with an absorbance edge up to 498 nm) and improves the separation efficiency of photoinduced charge-holes on the sample. In addition, the O-doping process can also enlarge the surface area of the sample. As expected, the O-doped g-C_3N_4 shows significant improvement in the photodegradation of methyl blue and photoevolution of H_2 under visible light irradiation. Moreover, and the catalyst can be recycled without appreciable loss in activity, as shown in Figure 16. Other authors state that the presence of heteroatoms in the synthesis process, even not being retained in the final product, can significantly change the textural structure and thus the photoactivity of g-C_3N_4 (e.g., g-C_3N_4 synthesized from thiourea exhibits a much higher H_2 production rate than the product prepared from dicyanamide or urea).[107]

Another interesting route for improving the photoactivity is the incorporation of metal ions into the framework of g-C_3N_4 (thus producing an organic−metal hybrid material), as the metal components can strongly modify the electronic properties of g-C_3N_4 and offer additional functionalities to the material. Although the detailed formation mechanism is not yet fully understood, metal ions (e.g., Fe^{3+}, Zn^{2+}) can be incorporated into the framework of g-C_3N_4 to form an organic−inorganic hybrid material, through a simple soft-chemical method, without destroying the graphitic structure of the host, and no inorganic iron-containing compound is observed even with an iron percentage of 20%.[108] Samples obtained that way (e.g., 10 wt % Fe/g-C_3N_4) show enhanced photoactivity for the oxidative degradation of organic dyes, e.g. rhodamine B (RhB), and selective oxidation of benzene to phenol. Moreover, the sample can be regenerated and reused without appreciable loss of RhB degradation activity up to five cycles, as depicted in Figure 17, suggesting that the iron ions are well-fixed in the framework of g-C_3N_4.

Apart from the in situ incorporation, the metal ions can also be coordinated with the g-C_3N_4 by postsynthesis.[96,109] In brief, the preformed g-C_3N_4 powder is dispersed into a metal ion-containing salt solution and then the water is evaporated to yield a metal-containing g-C_3N_4 solid, which is finally treated at desired temperature (e.g., 300 °C) to yield the final product. Such materials show enhanced photoactivity compared to the untreated g-C_3N_4, due to the coordination of the metal ions. It is reported that the conversion of benzene oxidation reaction into phenol can be greatly increased from 2%, for the untreated mpg-C_3N_4, to 23%, for $FeCl_3$ incorporated mpg-C_3N_4 (10% $FeCl_3$/mpg-C_3N_4).[96] Other nontransition metals can also be used to modify the electronic properties of g-C_3N_4. For instance, the deposition of noble metals (e.g., Pt) on the surface of g-C_3N_4 promotes the reaction not only by modifying the electronic properties of the material, but also by interacting with the intermediate as a cocatalyst. It is suggested that in the water splitting reaction catalyzed by Pt/g-C_3N_4, the initially formed N−H bond can be transformed into a Pt−H bond. That enhances the photoactivity, as the splitting of a Pt−H bond is kinetically more favorable than that of a N−H bond.[98]

Tran et al. report that a scalable catalyst, mpg-CN_x−CoPi−H_2−CoCat composite, can be obtained by loading a cobalt-

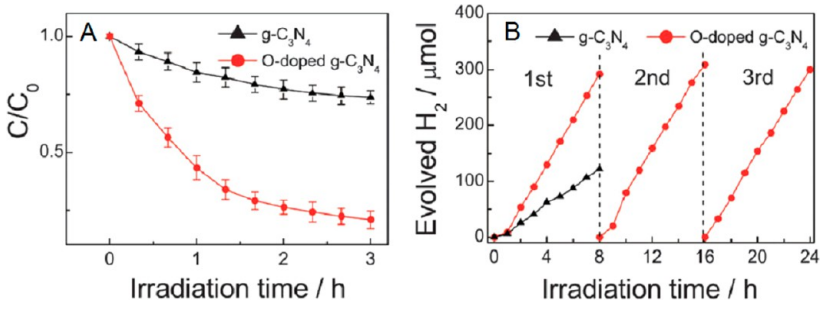

Figure 16. (A) Photodegradation of methyl blue and (B) photoevolution of H_2 on pure and O-doped g-C_3N_4, under visible light irradiation. Reprinted with permission from ref 103. Copyright 2012 Royal Society of Chemistry.

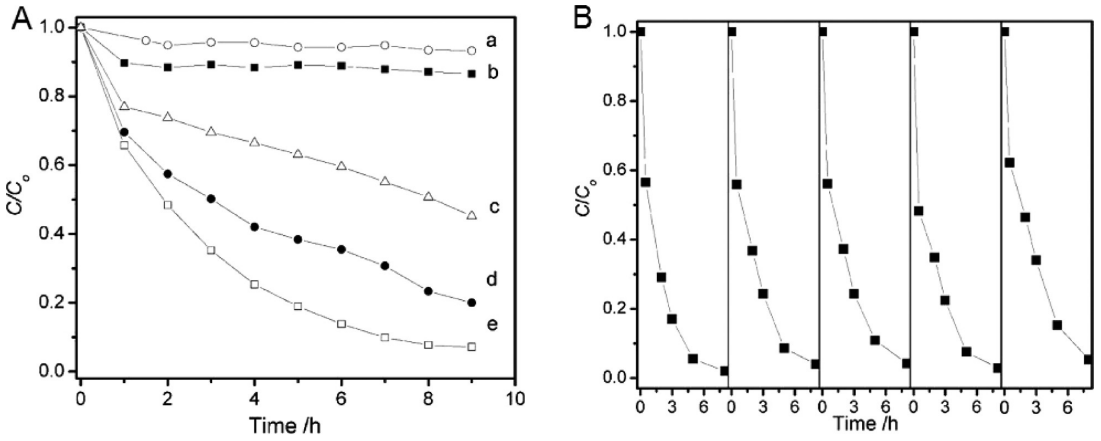

Figure 17. (A) Concentration changes of RhB (10 mM) as a function of reaction time under different conditions: (a) H_2O_2 (0.01 M); (b) Fe/g-C_3N_4 (40 mg); (c) Fe_2O_3 (40 mg)/H_2O_2 (0.01 M); (d) Fe/g-C_3N_4 (40 mg)/H_2O_2 (0.01 M); (e) Fe/g-C_3N_4 (40 mg)/H_2O_2 (0.01 M) under visible-light (λ > 420 nm) irradiation. (B) Cyclic runs of RhB (10 mM) degradation by H_2O_2 (0.05 M) activated by the Fe/g-C_3N_4 catalyst (40 mg). All reactions were carried out at neutral pH using the 10%-Fe/g-C_3N_4 catalyst. Reprinted with permission from ref 108. Copyright 2009 John Wiley & Sons.

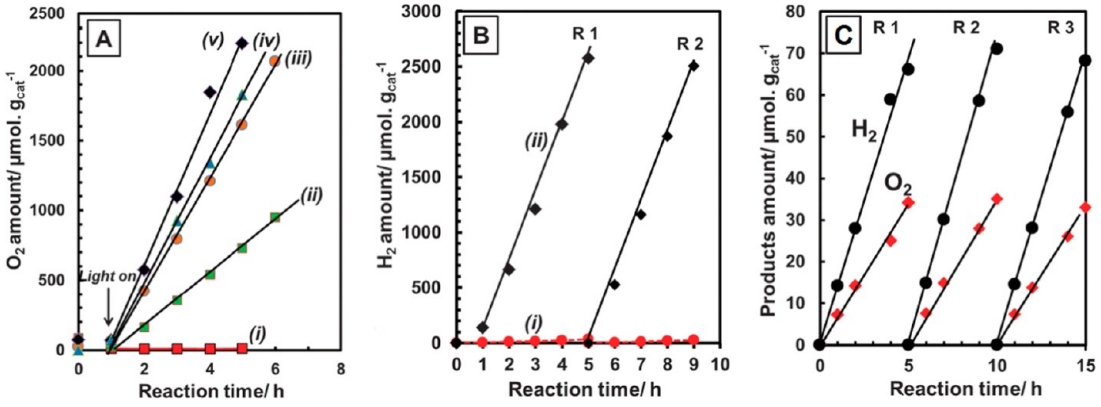

Figure 18. (A) Visible-light-driven water oxidation by mpg-CN_x-CoPi y% hybrid (y = 0, 1, 3, 5, and 10); (B) visible-light-driven hydrogen generation mediated by mpg-CN_x-H_2−CoCat photocatalyst, produced in situ from a mpg-CN_x-H_2−CoPi 10% composite, in a pH 7 phosphate buffer solution containing 10% (v/v) methanol; (C) visible-light-driven overall water splitting catalyzed by mpg-CN_x-CoPi-H_2−CoCat in pH 7 phosphate buffer solution without any scavengers.[110] Reprinted with permission from ref 110. Copyright 2013 Royal Society of Chemistry.

Scheme 3. Schematic Diagram Showing the Process of (A) the Photocatalytic Dye Degradation over a g-C_3N_4−Ag_3PO_4 Composite[a]; (B) H_2 Evolution Reaction over g-PAN/g-C_3N_4 Composites under Visible Light Irradiation[b]

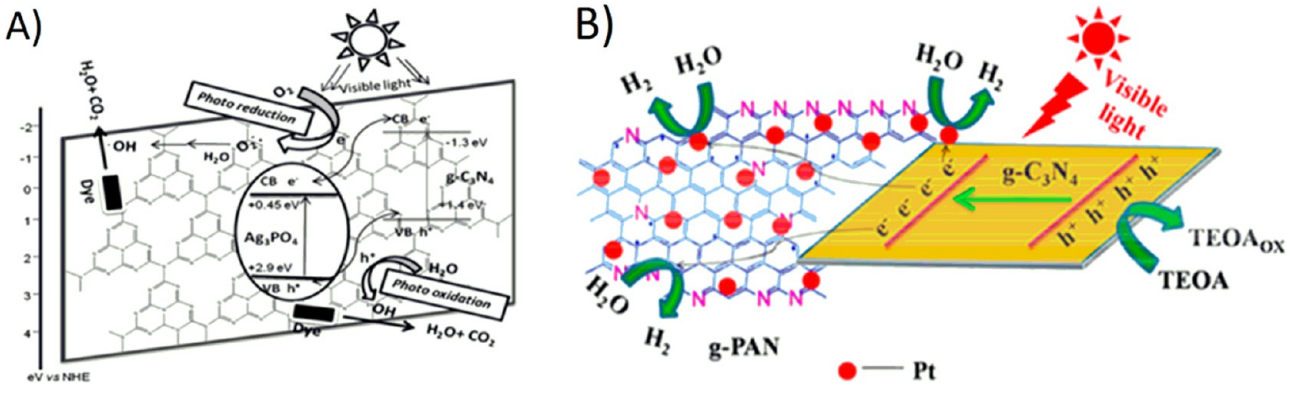

[a]Reprinted with permission from ref 111. Copyright 2013 Royal Society of Chemistry. [b]Reprinted with permission from ref 112. Copyright 2014 American Chemical Society.

oxide-phosphate (CoPi) water oxidation material onto the surface of a mpg-CN_x semiconductor.[110] The mpg-CN_x-CoPi hybrid can be evolved to mpg-CN_x-H_2−CoCat and subsequently to mpg-CN_x−CoPi−H_2−CoCat, after successive reactions. In brief, the mpg-CN_x-CoPi hybrid, active for water oxidation reaction, is gradually converted into an active hydrogen evolution reaction catalyst, mpg-CN_x-H_2−CoCat, when a hole scavenger, e.g. methanol, is used. The coexistence

of mpg-CN_x-CoPi and mpg-CN_x-H_2−CoCat results in the formation of a mpg-CN_x−CoPi−H_2−CoCat composite, which is active for the overall water splitting process, with reaction rates of 13.6 μmol g_{cat}^{-1} h^{-1} and 6.6 μmol g_{cat}^{-1} h^{-1} for H_2 and O_2 evolution, respectively. In each case (water oxidation into oxygen, hydrogen production or water splitting into hydrogen and oxygen), the corresponding catalyst shows a significantly enhanced activity compared to the untreated mpg-C_3N_4 catalyst, as depicted in Figure 18.

To decrease the recombination rate of photoinduced electron−hole pairs, a cocatalyst or other semiconductor materials can be loaded onto the surface of g-C_3N_4, to form a hybrid nanocomposite material, which can enhance the charge separation and photostability, due to their differentiated band positions. Both inorganic metal semiconductors and organic or polymer materials can be used to hybridize with g-C_3N_4; but the synthesis and the role in the reaction can be different. For the former, Shanker et al. report that the g-C_3N_4−Ag_3PO_4 nanocomposite photocatalyst can be prepared by in situ deposition of Ag_3PO_4 nanoparticles on the surface of a g-C_3N_4 sheet.[111] This composite shows improved photoactivity for the degradation of methyl orange under visible light irradiation, which is 5 and 3.5 times higher than pure g-C_3N_4 and Ag_3PO_4 respectively. Furthermore, the stability of Ag_3PO_4 can be greatly improved and the amount of silver effectively reduced. It is possible that the enhanced activity is due to smaller Ag_3PO_4 particle size, high surface area of the composite, or more critically, that a synergistic effect is induced between g-C_3N_4 and Ag_3PO_4. The electrons and holes induced by the visible light irradiation at the valence band (VB) and conduction band (CB) of Ag_3O_4 and g-C_3N_4 can then move freely under certain conditions, improving the charge separation efficiency of the photoinduced electron−hole pair, as shown in Scheme 3A. This is also true for other composites such as g-C_3N_4−AgX,[113] g-C_3N_4−TiO_2,[114] g-C_3N_4−ZnO,[115] and g-C_3N_4−$BiPO_4$.[116]

In the case of the polymer/g-C_3N_4 hybrid, the synthesis needs to be done more carefully, so that the precursor of the incorporated polymer will not react or interfere with the precursor of g-C_3N_4, during the synthesis process. Nevertheless, these composites are more interesting and applicable in practice, since they are cheap and environmentally friendly samples, and have the possibility to form nanosheet structured materials, with several advantages for photocatalysis, such as a large specific surface area, offering more reactive sites, and short diffusion distance, decreasing the recombination rate of photogenerated charge carriers.[117] A recent work from He and co-workers shows that a sheet-on-sheet g-PAN/g-C_3N_4 composite (where g-PAN is a graphitized polyacrylonitrile), which is entirely composed of environmentally friendly polymer materials, can be obtained by a facile one-step thermal condensation of PAN and melamine.[112] Photocatalytic tests show that the H_2 evolution rate increases from 0.7 μmol h^{-1} for the pristine g-C_3N_4, to 3.1 μmol h^{-1} for the 5.0 wt % g-PAN/g-C_3N_4 composite, and can be further improved to 37 μmol h^{-1} when a small amount of Pt is introduced, that is, Pt/5.0 wt % g-PAN/g-C_3N_4. It is proposed that the role of g-PAN in the reaction is to improve the interfacial charge transfer under visible light irradiation, e.g., transfer the photoinduced electrons from the CB of g-C_3N_4 to the Pt particles. That efficiently suppresses the recombination rate of the photogenarated charge-hole pairs and improves the catalytic activity, as illustrated in Scheme 3B.

5. CONCLUSIONS AND OUTLOOKS

This work summarizes the synthesis methods, physicochemical properties and applications of graphitic carbon nitride, g-C_3N_4, in heterogeneous catalysis. As a polymeric material, g-C_3N_4 can be prepared by polycondensation of a variety of precursors containing C/N/H and even O elements, and fabricated with different structures (bulk, supported, porous) and morphologies. The results of TGA measurements show that g-C_3N_4 can endure temperatures up to 600 °C and that the profiles are similar in inert or oxygen atmospheres, suggesting that g-C_3N_4 has high thermal stability and is inactive to oxygen. However, CO_2-TPD profiles suggest that the surface basicity of g-C_3N_4 is significantly affected by heating atmosphere, although no appreciable change in the crystalline structure is observed. Regarding the applications in catalysis, g-C_3N_4 is not only a good basic and metal-free catalyst for a variety of reactions, as reported in previous literature, but also an adequate reference material for differentiating the sites for oxygen activation over supported catalysts, and an excellent functional material in preparing small and stable metal nanoparticles for catalytic purposes.

In spite of the great achievements over the years, there are still many challenges in the applications of this material in catalysis. First, the structure stability and surface area of g-C_3N_4 need to be improved. It is known that g-C_3N_4 prepared by condensation route usually suffers from incomplete polycondensation, leading to different structures/composites from batch to batch, and the surface area of such prepared g-C_3N_4 material is low, which diminishes its catalytic activity. Although g-C_3N_4 with improved surface area can be obtained by a template method, the surface morphology and properties could be destroyed due to the drastic conditions used during the template etching process. Thus, the search for better, milder, and more reversible procedures to synthesize g-C_3N_4 with improved surface area is of crucial importance. Second, the physicochemical properties of g-C_3N_4 need to be further explored. Although g-C_3N_4 has been shown to be a good catalyst for several reactions, its actual role is not clear. The understanding of the physicochemical properties of g-C_3N_4 and its influence on the catalytic activity thus need to be correlated, in order to better understand the reaction and optimize the material. Finally, the most crucial is to improve the catalytic efficiency of g-C_3N_4 in the reactions. g-C_3N_4 is a covalent compound and its contribution to the reactions consists in the donation of electrons to the substrate, which requires the splitting and subsequent formation of the covalent bond during the reaction. This process is not easy, because of the high energy required for the splitting of a covalent bond, making the electron donation process slow and leading to low reaction rates. Therefore, the increase in surface energy and/or surface basicity of g-C_3N_4 is essential, to accelerate the rate of electron donation.

Apart from its role as a metal-free catalyst, it is also important to seek for new applications of g-C_3N_4 in catalysis, namely, as a functional material to graft metal nanoparticles in catalyst preparation, and as a reference material to produce catalysts to distinguish the oxygen activation sites. The finding of new uses should be based on the better understanding of the physicochemical properties of g-C_3N_4, which will undoubtedly widen its applications and lead to more exciting results.

AUTHOR INFORMATION

Corresponding Author

*E-mail: ciaczjj@gmail.com.

Author Contributions

The manuscript was written with the contributions of all authors. All authors approved the final version of the manuscript.

Notes

The authors declare no competing financial interests.

ACKNOWLEDGMENTS

J.Z. is grateful to prof. Kongyong Liew at South-central University for Nationalities for his contribution in the composition of the manuscript. Financial support from the National Science Foundation of China (21203254), the Scientific Research Foundation for Returned Scholars, Ministry of Education of China (BZY11055), and the National Demonstration Center of Experimental Teaching on ethnical pharmacy, South-Central University for Nationalities is greatly acknowledged. S.A.C.C. is grateful to Fundação para a Ciência e Tecnologia for Investigador FCT grant.

REFERENCES

(1) Cohen, M. L. Calculation of Bulk Moduli of Diamond and Zincblende Solids. *Phys. Rev. B* **1985**, *32*, 7988−7991.

(2) Liu, A. Y.; Cohen, M. L. Prediction of New Low Compressibility Solids. *Science* **1989**, *245*, 841−842.

(3) Liebig, J. Uber Einige Stickstoff - Verbindungen. *Ann. Pharm.* **1834**, *10*, 1−47.

(4) Wang, X.; Blechert, S.; Antonietti, M. Polymeric Graphitic Carbon Nitride for Heterogeneous Photocatalysis. *ACS Catal.* **2012**, *2*, 1596−1606.

(5) Thomas, A.; Fischer, A.; Goettmann, F.; Antonietti, M.; Muller, J. O.; Schlogl, R.; Carlsson, J. M. Graphitic Carbon Nitride Materials: Variation of Structure and Morphology and Their Use as Metal-Free Catalysts. *J. Mater. Chem.* **2008**, *18*, 4893−4908.

(6) Su, F.; Antonietti, M.; Wang, X. Mpg-C3n4 as a Solid Base Catalyst for Knoevenagel Condensations and Transesterification Reactions. *Catal. Sci. Technol.* **2012**, *2*, 1005−1009.

(7) Zhu, J. J.; Wei, Y. C.; Chen, W. K.; Zhao, Z.; Thomas, A. Graphitic Carbon Nitride as a Metal-Free Catalyst for No Decomposition. *Chem. Commun.* **2010**, *46*, 6965−6967.

(8) Wang, X. C.; Maeda, K.; Thomas, A.; Takanabe, K.; Xin, G.; Carlsson, J. M.; Domen, K.; Antonietti, M. A Metal-Free Polymeric Photocatalyst for Hydrogen Production from Water under Visible Light. *Nat. Mater.* **2009**, *8*, 76−80.

(9) Goettmann, F.; Thomas, A.; Antonietti, M. Metal-Free Activation CO_2 by Mesoporous Graphitic Carbon Nitride. *Angew. Chem., Int. Ed.* **2007**, *46*, 2717−2720.

(10) Huang, Z.; Li, F.; Chen, B.; Lu, T.; Yuan, Y.; Yuan, G. Well-Dispersed g-C_3N_4 Nanophases in Mesoporous Silica Channels and Their Catalytic Activity for Carbon Dioxide Activation and Conversion. *Appl. Catal., B* **2013**, *136−137*, 269−277.

(11) Jin, X.; Balasubramanian, V. V.; Selvan, S. T.; Sawant, D. P.; Chari, M. A.; Lu, G. Q.; Vinu, A. Highly Ordered Mesoporous Carbon Nitride Nanoparticles with High Nitrogen Content: A Metal-Free Basic Catalyst. *Angew. Chem., Int. Ed.* **2009**, *48*, 7884−7887.

(12) Zheng, Y.; Jiao, Y.; Chen, J.; Liu, J.; Liang, J.; Du, A.; Zhang, W.; Zhu, Z.; Smith, S. C.; Jaroniec, M.; Lu, G. Q.; Qiao, S. Z. Nanoporous Graphitic-C_3N_4@Carbon Metal-Free Electrocatalysts for Highly Efficient Oxygen Reduction. *J. Am. Chem. Soc.* **2011**, *133*, 20116−20119.

(13) Tian, J.; Ning, R.; Liu, Q.; Asiri, A. M.; Al-Youbi, A. O.; Sun, X. Three-Dimensional Porous Supramolecular Architecture from Ultrathin g-C_3N_4 Nanosheets and Reduced Graphene Oxide: Solution Self-Assembly Construction and Application as a Highly Efficient Metal-Free Electrocatalyst for Oxygen Reduction Reaction. *ACS Appl. Mater. Interfaces* **2013**, *6*, 1011−1017.

(14) Wang, X. C.; Maeda, K.; Chen, X. F.; Takanabe, K.; Domen, K.; Hou, Y. D.; Fu, X. Z.; Antonietti, M. Polymer Semiconductors for Artificial Photosynthesis: Hydrogen Evolution by Mesoporous Graphitic Carbon Nitride with Visible Light. *J. Am. Chem. Soc.* **2009**, *131*, 1680−1681.

(15) Shiraishi, Y.; Kanazawa, S.; Sugano, Y.; Tsukamoto, D.; Sakamoto, H.; Ichikawa, S.; Hirai, T. Highly Selective Production of Hydrogen Peroxide on Graphitic Carbon Nitride (g-C_3N_4) Photocatalyst Activated by Visible Light. *ACS Catal.* **2014**, *4*, 774−780.

(16) Ge, L.; Zuo, F.; Liu, J.; Ma, Q.; Wang, C.; Sun, D.; Bartels, L.; Feng, P. Synthesis and Efficient Visible Light Photocatalytic Hydrogen Evolution of Polymeric g-C_3N_4 Coupled with Cds Quantum Dots. *J. Phys. Chem. C* **2012**, *116*, 13708−13714.

(17) Bai, X.; Wang, L.; Zong, R.; Zhu, Y. Photocatalytic Activity Enhanced Via g-C_3N_4 Nanoplates to Nanorods. *J. Phys. Chem. C* **2013**, *117*, 9952−9961.

(18) Wang, Y.; Wang, X.; Antonietti, M. Polymeric Graphitic Carbon Nitride as a Heterogeneous Organocatalyst: From Photochemistry to Multipurpose Catalysis to Sustainable Chemistry. *Angew. Chem., Int. Ed.* **2012**, *51*, 68−89.

(19) Zheng, Y.; Liu, J.; Liang, J.; Jaroniec, M.; Qiao, S. Z. Graphitic Carbon Nitride Materials: Controllable Synthesis and Applications in Fuel Cells and Photocatalysis. *Energy Environ. Sci.* **2012**, *5*, 6717−6731.

(20) Li, X.-H.; Antonietti, M. Metal Nanoparticles at Mesoporous N-Doped Carbons and Carbon Nitrides: Functional Mott-Schottky Heterojunctions for Catalysis. *Chem. Soc. Rev.* **2013**, *42*, 6593−6604.

(21) Su, D. S.; Zhang, J.; Frank, B.; Thomas, A.; Wang, X. C.; Paraknowitsch, J.; Schlogl, R. Metal-Free Heterogeneous Catalysis for Sustainable Chemistry. *ChemSusChem* **2010**, *3*, 169−180.

(22) Maya, L.; Cole, D. R.; Hagaman, E. W. Carbon−Nitrogen Pyrolyzates: Attempted Preparation of Carbon Nitride. *J. Am. Ceram. Soc.* **1991**, *74*, 1686−1688.

(23) Nesting, D. C.; Badding, J. V. High-Pressure Synthesis of sp^2-Bonded Carbon Nitrides. *Chem. Mater.* **1996**, *8*, 1535−1539.

(24) Wehrstedt, K.-D.; Wildner, W.; Güthner, T.; Holzrichter, K.; Mertschenk, B.; Ulrich, A. Safe Transport of Cyanamide. *J. Hazard. Mater.* **2009**, *170*, 829−835.

(25) Xu, J.; Wu, H.-T.; Wang, X.; Xue, B.; Li, Y.-X.; Cao, Y. A New and Environmentally Benign Precursor for the Synthesis of Mesoporous g-C_3N_4 with Tunable Surface Area. *Phys. Chem. Chem. Phys.* **2013**, *15*, 4510−4517.

(26) Chen, X.; Zhang, J.; Fu, X.; Antonietti, M.; Wang, X. Fe- g-C_3N_4-Catalyzed Oxidation of Benzene to Phenol Using Hydrogen Peroxide and Visible Light. *J. Am. Chem. Soc.* **2009**, *131*, 11658−11659.

(27) Zhao, D. Y.; Feng, J. L.; Huo, Q. S.; Melosh, N.; Fredrickson, G. H.; Chmelka, B. F.; Stucky, G. D. Triblock Copolymer Syntheses of Mesoporous Silica with Periodic 50 to 300 Angstrom Pores. *Science* **1998**, *279*, 548−552.

(28) Thomas, A.; Goettmann, F.; Antonietti, M. Hard Templates for Soft Materials: Creating Nanostructured Organic Materials. *Chem. Mater.* **2008**, *20*, 738−755.

(29) Jun, Y. S.; Hong, W. H.; Antonietti, M.; Thomas, A. Mesoporous, 2D Hexagonal Carbon Nitride and Titanium Nitride/Carbon Composites. *Adv. Mater.* **2009**, *21*, 4270−4274.

(30) Kailasam, K.; Epping, J. D.; Thomas, A.; Losse, S.; Junge, H. Mesoporous Carbon Nitride-Silica Composites by a Combined Sol-Gel/Thermal Condensation Approach and Their Application as Photocatalysts. *Energy Environ. Sci.* **2011**, *4*, 4668−4674.

(31) Wang, Y.; Wang, X.; Antonietti, M.; Zhang, Y. Facile One-Pot Synthesis of Nanoporous Carbon Nitride Solids by Using Soft Templates. *ChemSusChem* **2010**, *3*, 435−439.

(32) Shen, W.; Ren, L.; Zhou, H.; Zhang, S.; Fan, W. Facile One-Pot Synthesis of Bimodal Mesoporous Carbon Nitride and Its Function as a Lipase Immobilization Support. *J. Mater. Chem.* **2011**, *21*, 3890−3894.

(33) Dong, F.; Wu, L.; Sun, Y.; Fu, M.; Wu, Z.; Lee, S. C. Efficient Synthesis of Polymeric g-C_3N_4 Layered Materials as Novel Efficient Visible Light Driven Photocatalysts. *J. Mater. Chem.* **2011**, *21*, 15171−15174.
(34) Zou, X.-X.; Li, G.-D.; Wang, Y.-N.; Zhao, J.; Yan, C.; Guo, M.-Y.; Li, L.; Chen, J.-S. Direct Conversion of Urea into Graphitic Carbon Nitride over Mesoporous TiO_2 Spheres under Mild Condition. *Chem. Commun.* **2011**, *47*, 1066−1068.
(35) Dai, H.; Gao, X.; Liu, E.; Yang, Y.; Hou, W.; Kang, L.; Fan, J.; Hu, X. Synthesis and Characterization of Graphitic Carbon Nitride Sub-Microspheres Using Microwave Method under Mild Condition. *Diamond Relat. Mater.* **2013**, *38*, 109−117.
(36) Lotsch, B. V.; Schnick, W. Thermal Conversion of Guanylurea Dicyanamide into Graphitic Carbon Nitride Via Prototype Cnx Precursors. *Chem. Mater.* **2005**, *17*, 3976−3982.
(37) Lotsch, B. V.; Schnick, W. From Triazines to Heptazines: Novel Nonmetal Tricyanomelaminates as Precursors for Graphitic Carbon Nitride Materials. *Chem. Mater.* **2006**, *18*, 1891−1900.
(38) Kroke, E.; Schwarz, M.; Horath-Bordon, E.; Kroll, P.; Noll, B.; Norman, A. D. Tri-S-Triazine Derivatives. Part I. From Trichloro-Tri-S-Triazine to Graphitic C_3N_4 Structures. *New J. Chem.* **2002**, *26*, 508−512.
(39) Matsumoto, S.; Xie, E. Q.; Izumi, F. On the Validity of the Formation of Crystalline Carbon Nitrides, C_3N_4. *Diamond Relat. Mater.* **1999**, *8*, 1175−1182.
(40) Semencha, A. V.; Blinov, L. N. Theoretical Prerequisites, Problems, and Practical Approaches to the Preparation of Carbon Nitride: A Review. *Glass Phys. Chem.* **2010**, *36*, 199−208.
(41) Bojdys, M. J. On New Allotropes and Nanostructures of Carbon Nitrides. Ph.D. Dissertation, Universitätsbibliothek Potsdam & Max-Planck Institute of Colloids and Interfaces, Potsdam, Germany, 2009.
(42) Zhang, Y. J.; Thomas, A.; Antonietti, M.; Wang, X. C. Activation of Carbon Nitride Solids by Protonation: Morphology Changes, Enhanced Ionic Conductivity, and Photoconduction Experiments. *J. Am. Chem. Soc.* **2009**, *131*, 50−51.
(43) Goettmann, F.; Fischer, A.; Antonietti, M.; Thomas, A. Metal-Free Catalysis of Sustainable Friedel-Crafts Reactions: Direct Activation of Benzene by Carbon Nitrides to Avoid the Use of Metal Chlorides and Halogenated Compounds. *Chem. Commun.* **2006**, 4530−4532.
(44) Wang, Y.; Li, H.; Yao, J.; Wang, X.; Antonietti, M. Synthesis of Boron Doped Polymeric Carbon Nitride Solids and Their Use as Metal-Free Catalysts for Aliphatic C-H Bond Oxidation. *Chem. Sci.* **2011**, *2*, 446−450.
(45) Roeser, J.; Kailasam, K.; Thomas, A. Covalent Triazine Frameworks as Heterogeneous Catalysts for the Synthesis of Cyclic and Linear Carbonates from Carbon Dioxide and Epoxides. *ChemSusChem* **2012**, *5*, 1793−1799.
(46) Wang, T.; Kailasam, K.; Xiao, P.; Chen, G.; Chen, L.; Wang, L.; Li, J.; Zhu, J. Adsorption Removal of Organic Dyes on Covalent Triazine Framework (CTF). *Microporous Mesoporous Mater.* **2014**, *187*, 63−70.
(47) Pietrzak, R.; Wachowska, H.; Nowicki, P. Preparation of Nitrogen-Enriched Activated Carbons from Brown Coal. *Energy Fuels* **2006**, *20*, 1275−1280.
(48) Grzybek, T.; Klinik, J.; Samojeden, B.; Suprun, V.; Papp, H. Nitrogen-Promoted Active Carbons as DeNO(x) Catalysts−1. The Influence of Modification Parameters on the Structure and Catalytic Properties. *Catal. Today* **2008**, *137*, 228−234.
(49) Wang, Y.; Di, Y.; Antonietti, M.; Li, H.; Chen, X.; Wang, X. Excellent Visible-Light Photocatalysis of Fluorinated Polymeric Carbon Nitride Solids. *Chem. Mater.* **2010**, *22*, 5119−5121.
(50) Liu, G.; Niu, P.; Sun, C.; Smith, S. C.; Chen, Z.; Lu, G. Q.; Cheng, H.-M. Unique Electronic Structure Induced High Photoreactivity of Sulfur-Doped Graphitic C_3N_4. *J. Am. Chem. Soc.* **2010**, *132*, 11642−11648.
(51) Zhang, Y.; Mori, T.; Ye, J.; Antonietti, M. Phosphorus-Doped Carbon Nitride Solid: Enhanced Electrical Conductivity and Photocurrent Generation. *J. Am. Chem. Soc.* **2010**, *132*, 6294−6295.
(52) Zhu, J. J.; Thomas, A. Perovskite-Type Mixed Oxides as Catalytic Material for NO Removal. *Appl. Catal,. B* **2009**, *92*, 225−233.
(53) Zhu, J. J.; Mao, D. H.; Li, J.; Xie, X. F.; Yang, X. G.; Wu, Y. Recycle - New Possible Mechanism of No Decomposition over Perovskite(-Like) Oxides. *J. Mol. Catal. A: Chem.* **2005**, *233*, 29−34.
(54) Zhu, J. J.; Yang, X. G.; Xu, X. L.; Wei, K. M. Active Site Structure of No Decomposition on Perovskite(-Like) Oxides: An Investigation from Experiment and Density Functional Theory. *J. Phys. Chem. C* **2007**, *111*, 1487−1490.
(55) Sokolovskii, V. D. Principles of Oxidative Catalysis on Solid Oxides. *Catal. Rev.* **1990**, *32*, 1−49.
(56) Schubert, M. M.; Hackenberg, S.; van Veen, A. C.; Muhler, M.; Plzak, V.; Behm, R. J. CO Oxidation over Supported Gold Catalysts-"Inert" and "Active" Support Materials and Their Role for the Oxygen Supply During Reaction. *J. Catal.* **2001**, *197*, 113−122.
(57) Yan, Z.; Chinta, S.; Mohamed, A. A.; Fackler, J. P.; Goodman, D. W. The Role of F-Centers in Catalysis by Au Supported on MgO. *J. Am. Chem. Soc.* **2005**, *127*, 1604−1605.
(58) Haruta, M.; Date, M. Advances in the Catalysis of Au Nanoparticles. *Appl. Catal. A-Gen.* **2001**, *222*, 427−437.
(59) Liu, H.; Kozlov, A. I.; Kozlova, A. P.; Shido, T.; Asakura, K.; Iwasawa, Y. Active Oxygen Species and Mechanism for Low-Temperature CO Oxidation Reaction on a TiO_2-Supported Au Catalyst Prepared from $Au(PPh_3)(NO_3)$ and as-Precipitated Titanium Hydroxide. *J. Catal.* **1999**, *185*, 252−264.
(60) Okumura, M.; Coronado, J. M.; Soria, J.; Haruta, M.; Conesa, J. C. EPR Study of CO and O_2 Interaction with Supported Au Catalysts. *J. Catal.* **2001**, *203*, 168−174.
(61) Liu, Z. P.; Gong, X. Q.; Kohanoff, J.; Sanchez, C.; Hu, P. Catalytic Role of Metal Oxides in Gold-Based Catalysts: A First Principles Study of CO Oxidation on TiO_2 Supported Au. *Phys. Rev. Lett.* **2003**, *91*, 266102−266105.
(62) Haruta, M. Catalysis−Gold Rush. *Nature* **2005**, *437*, 1098−1099.
(63) Widmann, D.; Behm, R. J. Activation of Molecular Oxygen and the Nature of the Active Oxygen Species for CO Oxidation on Oxide Supported Au Catalysts. *Acc. Chem. Res.* **2014**, *47*, 740−749.
(64) Zhu, J. J.; Carabineiro, S. A. C.; Shan, D.; Faria, J. L.; Zhu, Y. J.; Figueiredo, J. L. Oxygen Activation Sites in Gold and Iron Catalysts Supported on Carbon Nitride and Activated Carbon. *J. Catal.* **2010**, *274*, 207−214.
(65) Mallat, T.; Baiker, A. Oxidation of Alcohols with Molecular Oxygen on Solid Catalysts. *Chem. Rev.* **2004**, *104*, 3037−3058.
(66) Corma, A.; Garcia, H. Supported Gold Nanoparticles as Catalysts for Organic Reactions. *Chem. Soc. Rev.* **2008**, *37*, 2096−2126.
(67) Zhu, J. J.; Faria, J. L.; Figueiredo, J. L.; Thomas, A. Reaction Mechanism of Aerobic Oxidation of Alcohols Conducted on Activated-Carbon-Supported Cobalt Oxide Catalysts. *Chem.—Eur. J.* **2011**, *17*, 7112−7117.
(68) Xiao, P.; zhao, Y. X.; Wang, T.; Zhan, Y. Y.; Wang, H. H.; Li, J. L.; Thomas, A.; Zhu, J. J. Polymeric Carbon Nitride/Mesoporous Silica Composites as Catalyst Support for Au and Pt Nanoparticles. *Chem.—Eur. J.* **2014**, *20*, 2872−2878.
(69) Turner, M.; Golovko, V. B.; Vaughan, O. P. H.; Abdulkin, P.; Berenguer-Murcia, A.; Tikhov, M. S.; Johnson, B. F. G.; Lambert, R. M. Selective Oxidation with Dioxygen by Gold Nanoparticle Catalysts Derived from 55-Atom Clusters. *Nature* **2008**, *454*, 981−984.
(70) Zhu, Y.; Zaera, F. Selectivity in the Catalytic Hydrogenation of Cinnamaldehyde Promoted by Pt/SiO_2 as a Function of Metal Nanoparticle Size. *Catal. Sci. Technol.* **2014**, *4*, 955−962.
(71) Lee, I.; Delbecq, F.; Morales, R.; Albiter, M. A.; Zaera, F. Tuning Selectivity in Catalysis by Controlling Particle Shape. *Nat. Mater.* **2009**, *8*, 132−138.
(72) Prashar, A. K.; Mayadevi, S.; Nandini Devi, R. Effect of Particle Size on Selective Hydrogenation of Cinnamaldehyde by Pt Encapsulated in Mesoporous Silica. *Catal. Commun.* **2012**, *28*, 42−46.
(73) Alivisatos, A. P. Semiconductor Clusters, Nanocrystals, and Quantum Dots. *Science* **1996**, *271*, 933−937.

(74) Zhu, J.; Wang, T.; Xu, X.; Xiao, P.; Li, J. Pt Nanoparticles Supported on SBA-15: Synthesis, Characterization and Applications in Heterogeneous Catalysis. *Appl. Catal., B* **2013**, *130−131*, 197−217.
(75) Lee, B.; Ma, Z.; Zhang, Z.; Park, C.; Dai, S. Influences of Synthesis Conditions and Mesoporous Structures on the Gold Nanoparticles Supported on Mesoporous Silica Hosts. *Microporous Mesoporous Mater.* **2009**, *122*, 160−167.
(76) Konova, P.; Naydenov, A.; Venkov, C.; Mehandjiev, D.; Andreeva, D.; Tabakova, T. Activity and Deactivation of Au/TiO_2 Catalyst in Co Oxidation. *J. Mol. Catal. A: Chem.* **2004**, *213*, 235−240.
(77) Chan-Thaw, C. E.; Villa, A.; Katekomol, P.; Su, D. S.; Thomas, A.; Prati, L. Covalent Triazine Framework as Catalytic Support for Liquid Phase Reaction. *Nano Lett.* **2010**, *10*, 537−541.
(78) Yang, C.-m.; Kalwei, M.; Schüth, F.; Chao, K.-j. Gold Nanoparticles in SBA-15 Showing Catalytic Activity in CO Oxidation. *Appl. Catal., A* **2003**, *254*, 289−296.
(79) Joo, S. H.; Park, J. Y.; Tsung, C.-K.; Yamada, Y.; Yang, P.; Somorjai, G. A. Thermally Stable Pt/Mesoporous Silica Core-Shell Nanocatalysts for High-Temperature Reactions. *Nat. Mater.* **2009**, *8*, 126−131.
(80) Chan-Thaw, C. E.; Villa, A.; Prati, L.; Thomas, A. Triazine-Based Polymers as Nanostructured Supports for the Liquid-Phase Oxidation of Alcohols. *Chem.—Eur. J.* **2011**, *17*, 1052−1057.
(81) Chan-Thaw, C. E.; Villa, A.; Veith, G. M.; Kailasam, K.; Adamczyk, L. A.; Unocic, R. R.; Prati, L.; Thomas, A. Influence of Periodic Nitrogen Functionality on the Selective Oxidation of Alcohols. *Chem.—Asian J.* **2012**, *7*, 387−393.
(82) Li, Y.; Xu, X.; Zhang, P.; Gong, Y.; Li, H.; Wang, Y. Highly Selective $Pd@mpg-C_3N_4$ Catalyst for Phenol Hydrogenation in Aqueous Phase. *RSC Adv.* **2013**, *3*, 10973−10982.
(83) Li, Y.; Gong, Y.; Xu, X.; Zhang, P.; Li, H.; Wang, Y. A Practical and Benign Synthesis of Amines through $Pd@Mpg-C_3N_4$ Catalyzed Reduction of Nitriles. *Catal. Commun.* **2012**, *28*, 9−12.
(84) Wang, Y.; Yao, J.; Li, H.; Su, D.; Antonietti, M. Highly Selective Hydrogenation of Phenol and Derivatives over a Pd@Carbon Nitride Catalyst in Aqueous Media. *J. Am. Chem. Soc.* **2011**, *133*, 2362−2365.
(85) Deng, D.; Yang, Y.; Gong, Y.; Li, Y.; Xu, X.; Wang, Y. Palladium Nanoparticles Supported on $mpg-C_3N_4$ as Active Catalyst for Semihydrogenation of Phenylacetylene under Mild Conditions. *Green Chem.* **2013**, *15*, 2525−2531.
(86) Chang, C.; Fu, Y.; Hu, M.; Wang, C.; Shan, G.; Zhu, L. Photodegradation of Bisphenol a by Highly Stable Palladium-Doped Mesoporous Graphite Carbon Nitride ($Pd/mpg-C_3N_4$) under Simulated Solar Light Irradiation. *Appl. Catal., B* **2013**, *142−143*, 553−560.
(87) Li, X.-H.; Wang, X.; Antonietti, M. Mesoporous $g-C_3N_4$ Nanorods as Multifunctional Supports of Ultrafine Metal Nanoparticles: Hydrogen Generation from Water and Reduction of Nitrophenol with Tandem Catalysis in One Step. *Chem. Sci.* **2012**, *3*, 2170−2174.
(88) Cui, Y.; Ding, Z.; Liu, P.; Antonietti, M.; Fu, X.; Wang, X. Metal-free Activation of H_2O_2 by $g-C_3N_4$ under Visible Light Irradiation for the Degradation of Organic Pollutants. *Phys. Chem. Chem. Phys.* **2012**, *14*, 1455−1462.
(89) Cheng, N.; Tian, J.; Liu, Q.; Ge, C.; Qusti, A. H.; Asiri, A. M.; Al-Youbi, A. O.; Sun, X. Au-Nanoparticle-Loaded Graphitic Carbon Nitride Nanosheets: Green Photocatalytic Synthesis and Application toward the Degradation of Organic Pollutants. *ACS Appl. Mater. Interfaces* **2013**, *5*, 6815−6819.
(90) Chang, C.; Zhu, L.; Wang, S.; Chu, X.; Yue, L. Novel Mesoporous Graphite Carbon Nitride/BiOI Heterojunction for Enhancing Photocatalytic Performance Under Visible-Light Irradiation. *ACS Appl. Mater. Interfaces* **2014**, *6*, 5083−5093.
(91) Lewis, N. S.; Nocera, D. G. Powering the planet: Chemical challenges in solar energy utilization. *Proc. Natl. Acad. Sci. U.S.A.* **2006**, *103*, 15729−15735.
(92) Cook, T. R.; Dogutan, D. K.; Reece, S. Y.; Surendranath, Y.; Teets, T. S.; Nocera, D. G. Solar Energy Supply and Storage for the Legacy and Nonlegacy Worlds. *Chem. Rev.* **2010**, *110*, 6474−6502.
(93) Liu, J.; Zhang, Y.; Lu, L.; Wu, G.; Chen, W. Self-regenerated Solar-driven Pphotocatalytic Water-splitting by Urea Derived Graphitic Carbon Nitride with Platinum Nanoparticles. *Chem. Commun.* **2012**, *48*, 8826−8828.
(94) Mao, J.; Peng, T.; Zhang, X.; Li, K.; Ye, L.; Zan, L. Effect of Graphitic Carbon Nitride Microstructures on the Activity and Selectivity of Photocatalytic CO_2 Reduction under Visible Light. *Catal. Sci. Technol.* **2013**, *3*, 1253−1260.
(95) Lin, J.; Pan, Z.; Wang, X. Photochemical Reduction of CO_2 by Graphitic Carbon Nitride Polymers. *ACS Sustainable Chem. Eng.* **2013**, *2*, 353−358.
(96) Zhang, P.; Gong, Y.; Li, H.; Chen, Z.; Wang, Y. Selective Oxidation of Benzene to Phenol by $FeCl_3/mpg-C_3N_4$ Hybrids. *RSC Adv.* **2013**, *3*, 5121−5126.
(97) Wang, X.; Maeda, K.; Thomas, A.; Takanabe, K.; Xin, G.; Carlsson, J. M.; Domen, K.; Antonietti, M. A Metal-free Polymeric Photocatalyst for Hydrogen Production from Water under Visible Light. *Nat. Mater.* **2009**, *8*, 76−80.
(98) Maeda, K.; Wang, X.; Nishihara, Y.; Lu, D.; Antonietti, M.; Domen, K. Photocatalytic Activities of Graphitic Carbon Nitride Powder for Water Reduction and Oxidation under Visible Light. *J. Phys. Chem. C* **2009**, *113*, 4940−4947.
(99) Wang, X.; Maeda, K.; Chen, X.; Takanabe, K.; Domen, K.; Hou, Y.; Fu, X.; Antonietti, M. Polymer Semiconductors for Artificial Photosynthesis: Hydrogen Evolution by Mesoporous Graphitic Carbon Nitride with Visible Light. *J. Am. Chem. Soc.* **2009**, *131*, 1680−1681.
(100) Zhang, M.; Xu, J.; Zong, R.; Zhu, Y. Enhancement of Visible Light Photocatalytic Activities via Porous Structure of $g-C_3N_4$. *Appl. Catal,. B* **2014**, *147*, 229−235.
(101) Xu, J.; Wang, Y.; Zhu, Y. Nanoporous Graphitic Carbon Nitride with Enhanced Photocatalytic Performance. *Langmuir* **2013**, *29*, 10566−10572.
(102) Cui, Y.; Huang, J.; Fu, X.; Wang, X. Metal-free Photocatalytic Degradation of 4-Chlorophenol in Water by Mesoporous Carbon Nitride Semiconductors. *Catal. Sci. Technol.* **2012**, *2*, 1396−1402.
(103) Li, J.; Shen, B.; Hong, Z.; Lin, B.; Gao, B.; Chen, Y. A Facile Approach to Synthesize Novel Oxygen-doped $g-C_3N_4$ with Superior Visible-light Photoreactivity. *Chem. Commun.* **2012**, *48*, 12017−12019.
(104) Dong, G.; Zhao, K.; Zhang, L. Carbon Self-doping Induced High Electronic Conductivity and Photoreactivity of $g-C_3N_4$. *Chem. Commun.* **2012**, *48*, 6178−6180.
(105) Zhang, J.; Sun, J.; Maeda, K.; Domen, K.; Liu, P.; Antonietti, M.; Fu, X.; Wang, X. Sulfur-mediated Synthesis of Carbon Nitride: Band-gap Engineering and Improved Functions for Photocatalysis. *Energy Environ. Sci.* **2011**, *4*, 675−678.
(106) Yan, S. C.; Li, Z. S.; Zou, Z. G. Photodegradation of Rhodamine B and Methyl Orange over Boron-Doped g-C3N4 under Visible Light Irradiation. *Langmuir* **2010**, *26*, 3894−3901.
(107) Zhang, G.; Zhang, J.; Zhang, M.; Wang, X. Polycondensation of Thiourea into Carbon Nitride Semiconductors as Visible Light Photocatalysts. *J. Mater. Chem.* **2012**, *22*, 8083−8091.
(108) Wang, X.; Chen, X.; Thomas, A.; Fu, X.; Antonietti, M. Metal-Containing Carbon Nitride Compounds: A New Functional Organic−Metal Hybrid Material. *Adv. Mater.* **2009**, *21*, 1609−1612.
(109) Gao, H.; Yan, S.; Wang, J.; Zou, Z. Ion Coordination Significantly Enhances the Photocatalytic Activity of Graphitic-phase Carbon Nitride. *Dalton. Trans.* **2014**, *43*, 8178−8183.
(110) Lee, R.-L.; Tran, P. D.; Pramana, S. S.; Chiam, S. Y.; Ren, Y.; Meng, S.; Wong, L. H.; Barber, J. Assembling Graphitic-Carbon-Nitride with Cobalt-Oxide-Phosphate to Construct an Efficient Hybrid Photocatalyst for Water Splitting Application. *Catal. Sci. Technol.* **2013**, *3*, 1694−1698.
(111) Kumar, S.; Surendar, T.; Baruah, A.; Shanker, V. Synthesis of a Novel and Stable $g-C_3N_4-Ag_3PO_4$ Hybrid Nanocomposite Photocatalyst and Study of the Photocatalytic Activity under Visible Light Irradiation. *J. Mater. Chem. A* **2013**, *1*, 5333−5340.
(112) He, F.; Chen, G.; Yu, Y.; Hao, S.; Zhou, Y.; Zheng, Y. Facile Approach to Synthesize g-PAN/g-C3N4 Composites with Enhanced

Photocatalytic H2 Evolution Activity. *ACS Appl. Mater. Interfaces* **2014**, *6*, 7171−7179.
(113) Xu, H.; Yan, J.; Xu, Y.; Song, Y.; Li, H.; Xia, J.; Huang, C.; Wan, H. Novel Visible-Light-Driven AgX/graphite-like C_3N_4 (X = Br, I) Hybrid Materials with Synergistic Photocatalytic Activity. *Appl. Catal., B* **2013**, *129*, 182−193.
(114) Lu, X.; Wang, Q.; Cui, D. Preparation and Photocatalytic Properties of g-C_3N_4/TiO_2 Hybrid Composite. *J. Mater. Sci. Technol.* **2010**, *26*, 925−930.
(115) Liu, W.; Wang, M.; Xu, C.; Chen, S. Facile Synthesis of g-C_3N_4/ZnO Composite with Enhanced Visible Light Photooxidation and Photoreduction Properties. *Chem. Eng. J.* **2012**, *209*, 386−393.
(116) Pan, C.; Xu, J.; Wang, Y.; Li, D.; Zhu, Y. Dramatic Activity of C_3N_4/$BiPO_4$ Photocatalyst with Core/Shell Structure Formed by Self-Assembly. *Adv. Funct. Mater.* **2012**, *22*, 1518−1524.
(117) Niu, P.; Zhang, L.; Liu, G.; Cheng, H. M. Graphene-Like Carbon Nitride Nanosheets for Improved Photocatalytic Activities. *Adv. Funct. Mater.* **2012**, *22*, 4763−4770.